The Power of RF

The University of Nottingham

University of Nottingham

Sindhu Jammi
Tadas Pyragius
Thomas Bishop
Fabio Gentile
Jamie Johnson
Hans Marin-Florez
Mark Bason
Thomas Fernholz

FP7-ICT-601180

MatterWave

MatterWave Collaboration

Nottingham (Igor Lesanovsky et al.)
Be'er Scheva (Ron Folman et al.)
Heraklion (Wolf von Klitzing et al.)
Birmingham (Kai Bongs, Vincent Boyer et al.)
Trieste (Andrea Trombettoni et al.)

EPSRC
Engineering and Physical Sciences Research Council

UK National
Quantum Technology Hub
Sensors and Metrology

Delta-T Devices

Outline

- **Measuring rotation**
  alternative views of the Sagnac effect
- **Radio-frequency dressed potentials**
  rotating frame, field polarizations,
  rings, tori, state-dependence and countertransport
- **A freebie – RF-dressed detection of clock states**
  non-destructive probing with lock-in
- **Driving clock transitions between rf-dressed states**
  fresh from the lab
- **Work in progress**
  ideas and issues

Georges Sagnac
1869-1928

A trick question

Two airplanes **leave** Singapore at the **same time**.

Airplane 1 travels eastward.
Airplane 2 travels westward.

Both airplanes **arrive** in Singapore at the **same time**.

Which trip took longer?

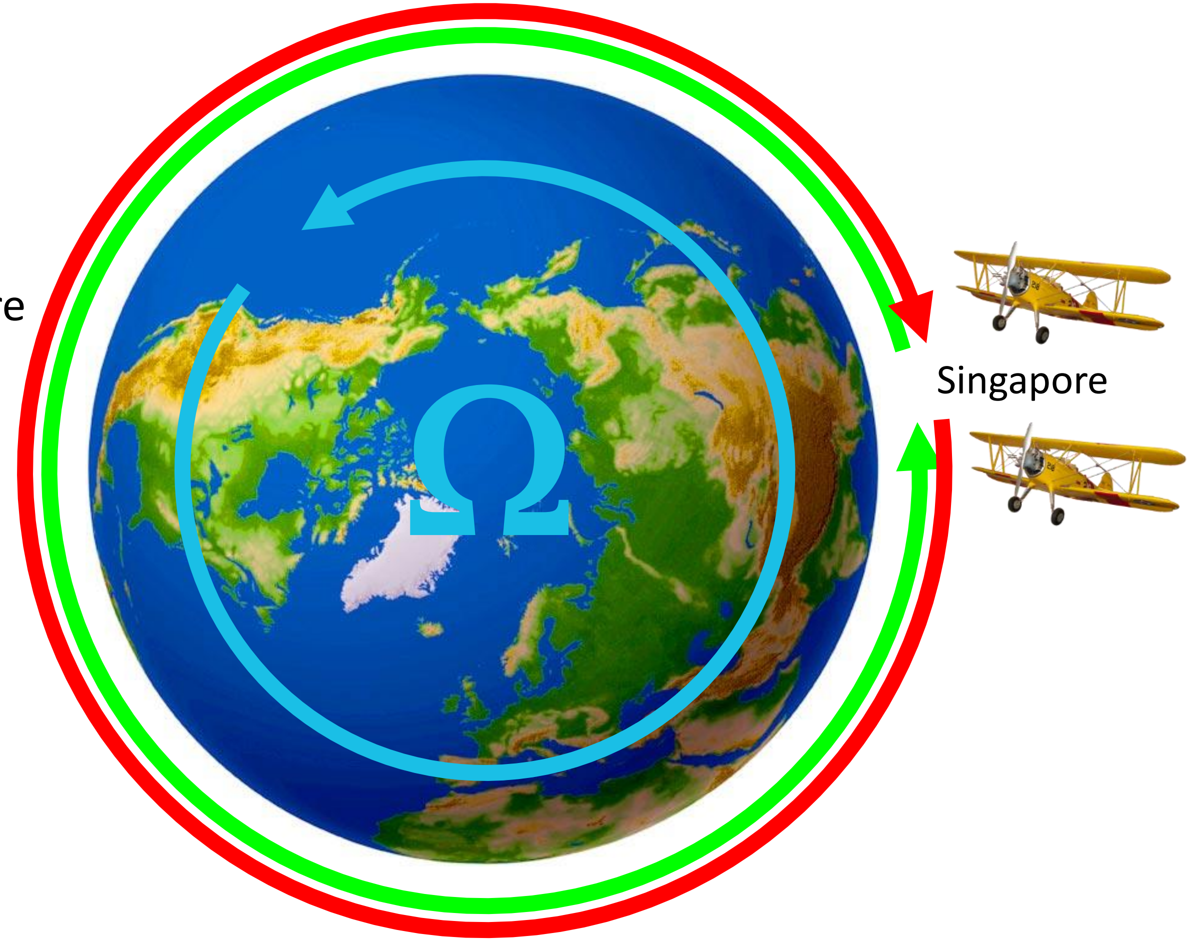

Hafele-Keating experiment

The University of Nottingham

Joseph C. Hafele   Richard E. Keating

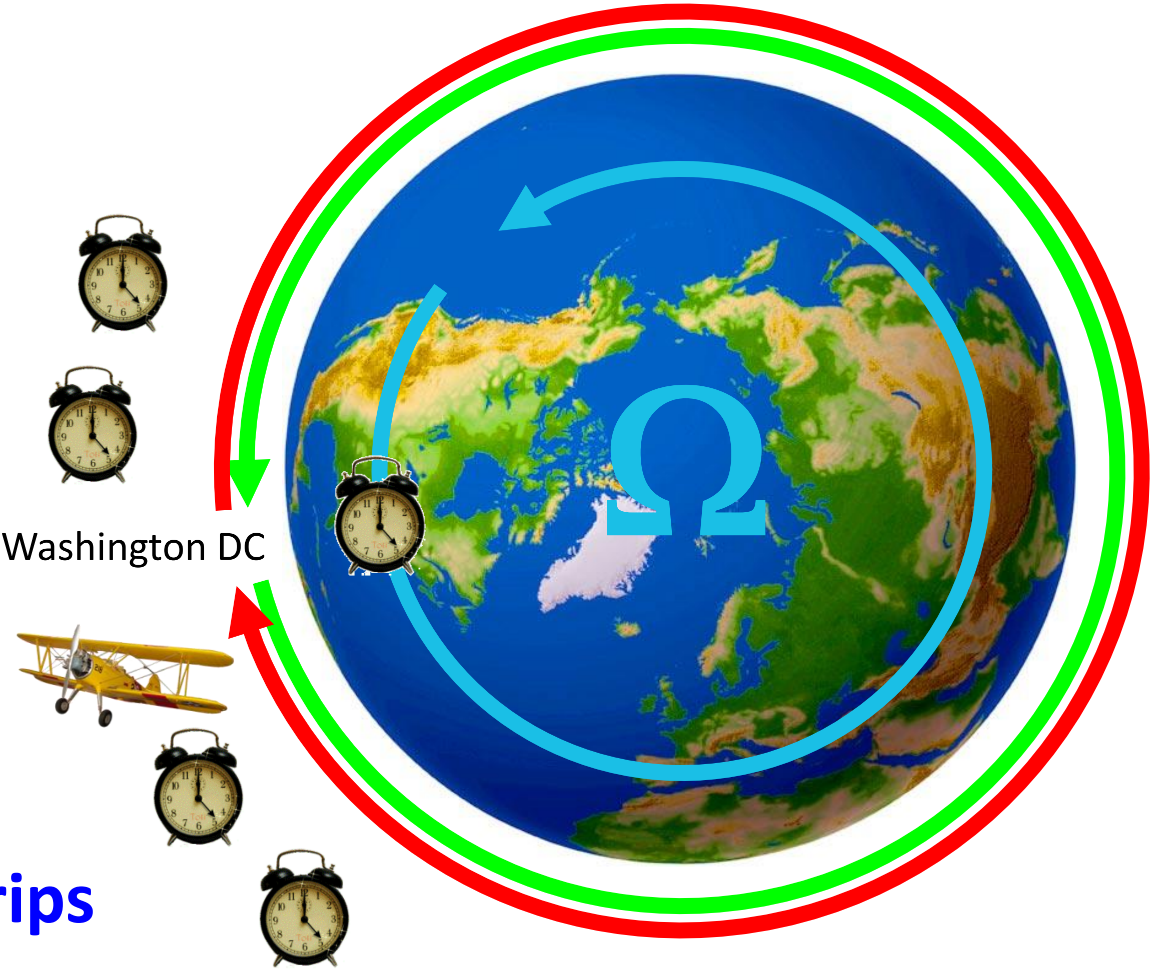

Several planes, two trips

Five atomic clocks

Hafele-Keating experiment

Joseph C. Hafele ? Richard E. Keating

Science **177**, 168pp (1972) & ibid. 166pp

Around-the-World Atomic Clocks: Observed Relativistic Time Gains

Abstract. *Four cesium beam clocks flown around the world on commercial jet flights during October 1971, once eastward and once westward, recorded directionally dependent time differences which are in good agreement with predictions of conventional relativity theory. Relative to the atomic time scale of the U.S. Naval Observatory, the flying clocks lost 59 ± 10 nanoseconds during the eastward trip and gained 273 ± 7 nanoseconds during the westward trip, where the errors are the corresponding standard deviations. These results provide an unambiguous empirical resolution of the famous clock "paradox" with macroscopic clocks.*

	Nanoseconds gained			
	Predicted			Measured
	Gravitational (general relativity)	**Kinematic** (special relativity)	**Total**	
Eastward	144 ± 14	−184 ± 18	−40 ± 23	−59 ± 10
Westward	179 ± 18	96 ± 10	275 ± 21	273 ± 7

Westward trips take longer!

Sagnac Effect

Circular path, radius R

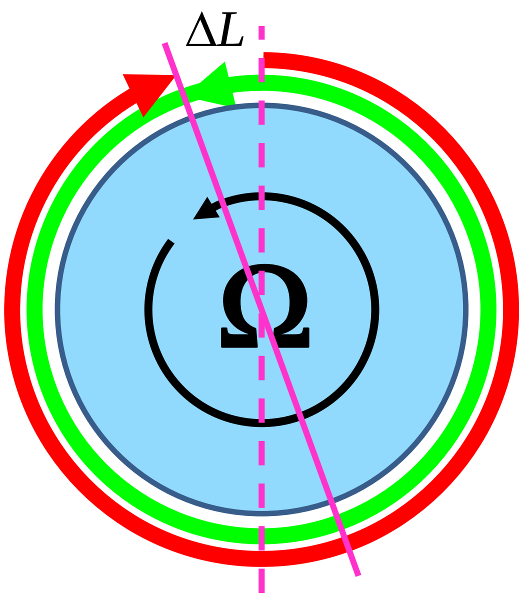

In an **inertial frame**, both trips take time T_0

The east/westward trips covers length $L_{E,W} = 2\pi R \pm \Delta L = 2\pi R \pm R\Omega T_0$

The average east/westward speed is $v_{E,W} = \frac{2\pi R}{T_0} \pm R\Omega$

According to special relativity, the travellers' **proper times** are:

$$T_{E,W} = T_0\sqrt{1-\left(\frac{v_{E,W}}{c}\right)^2} = T_0\sqrt{1-\left(\frac{2\pi R \pm R\Omega T_0}{cT_0}\right)^2}$$

Proper times expanded by orders of Ω

$$T_{E,W} \approx T_0\sqrt{1-\left(\frac{2\pi R}{cT_0}\right)^2} \mp \frac{2\pi R^2}{c^2\sqrt{1-\left(\frac{2\pi R}{cT_0}\right)^2}}\cdot\Omega - \frac{T_0}{2\left(\frac{c^2}{R^2}-\frac{4\pi^2}{T_0^{\,2}}\right)\sqrt{1-\left(\frac{2\pi R}{cT_0}\right)^2}}\cdot\Omega^2 \mp O(\Omega)^3$$

Sagnac Effect

Circular path, radius R

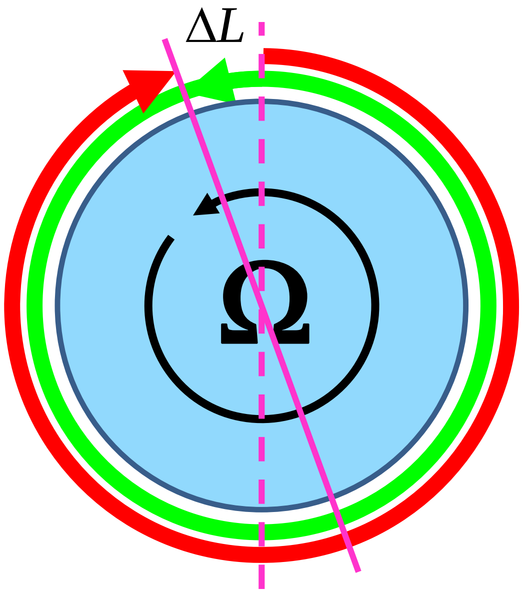

Time dilations for non-relativistic speeds, i.e. $\frac{2\pi R}{cT_0} << 1$

$$T_{E,W} \approx T_0 \mp \frac{2\pi R^2}{c^2} \cdot \Omega - \frac{R^2 T_0^{\ 2}}{2c^2} \cdot \Omega^2 \mp O(\Omega)^3$$

Proper time difference for non-relativistic speeds:

$$\Delta T = T_W - T_E \approx \frac{4A}{c^2} \cdot \Omega$$

Sagnac Phase of Matter waves

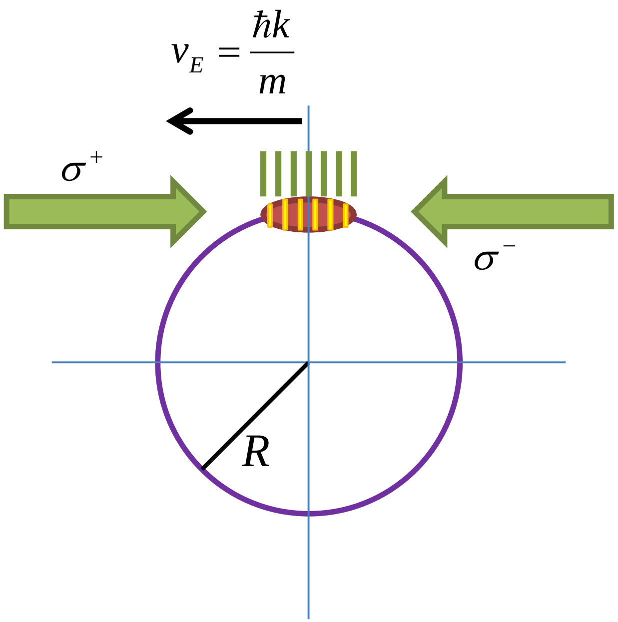

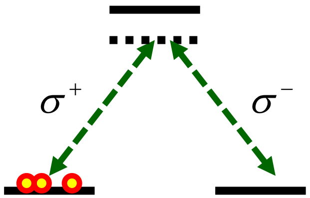

Sagnac Phase of Matter waves

The University of Nottingham

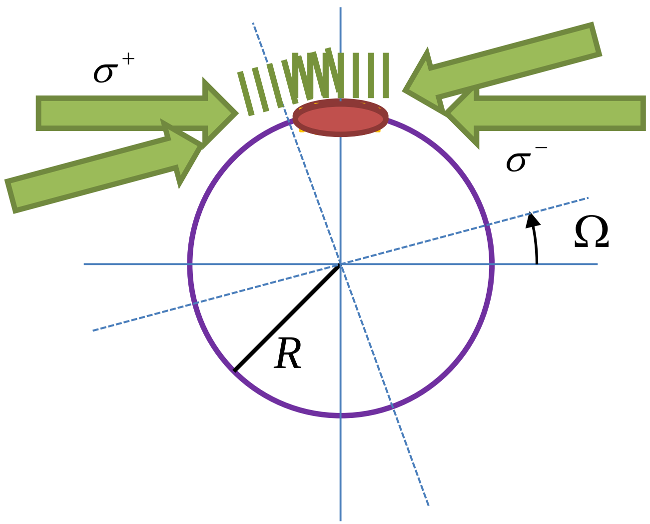

What is the relative phase shift between the two patterns?

Round trip time: $$T_0 = \frac{2\pi R}{v_{E,W}} = \frac{m\lambda}{\hbar} R$$

Pattern displacement: $$\Delta s = \Omega R \cdot T_0 = \frac{m\lambda}{\hbar} R^2 \Omega$$

Phase shift: $$\Delta\varphi = \frac{\Delta s}{\lambda/2} 2\pi = \frac{m}{\hbar} 4\pi R^2 \Omega$$

Compton frequency × **Proper time difference**

$$\boxed{\Delta\varphi = \frac{m}{\hbar} 4A\Omega = \frac{mc^2}{\hbar} \cdot \frac{4A\Omega}{c^2}}$$

Phase of a Quantum State

The University of Nottingham

Compton frequency $\times$ Proper time

$$\Psi_{\text{restframe}}(\tau) = \Psi(0) \cdot e^{i\omega_C\tau}$$

$$\Delta\varphi = \Delta(\omega_C\tau) \approx \boxed{\omega_C\Delta\tau} + \boxed{\Delta\omega_C\tau}$$

Sagnac phase

Atomic clock phase

Single Clock Sagnac Effect

The University of Nottingham

Microwave field – Ramsey Sequence
removes dynamic clock phase

Hyperfine splitting of ^{87}Rubidium
(nuclear spin precession)

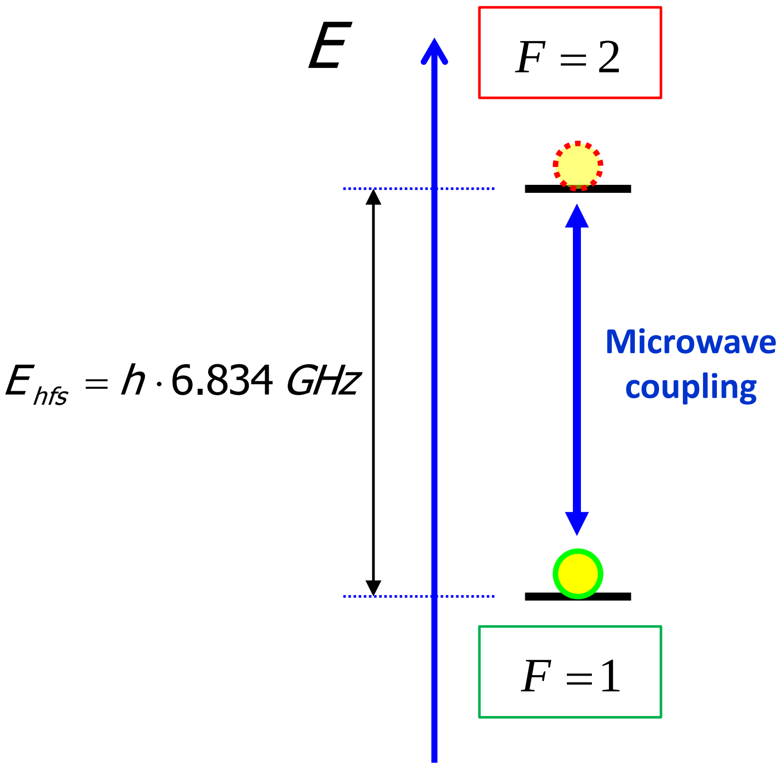

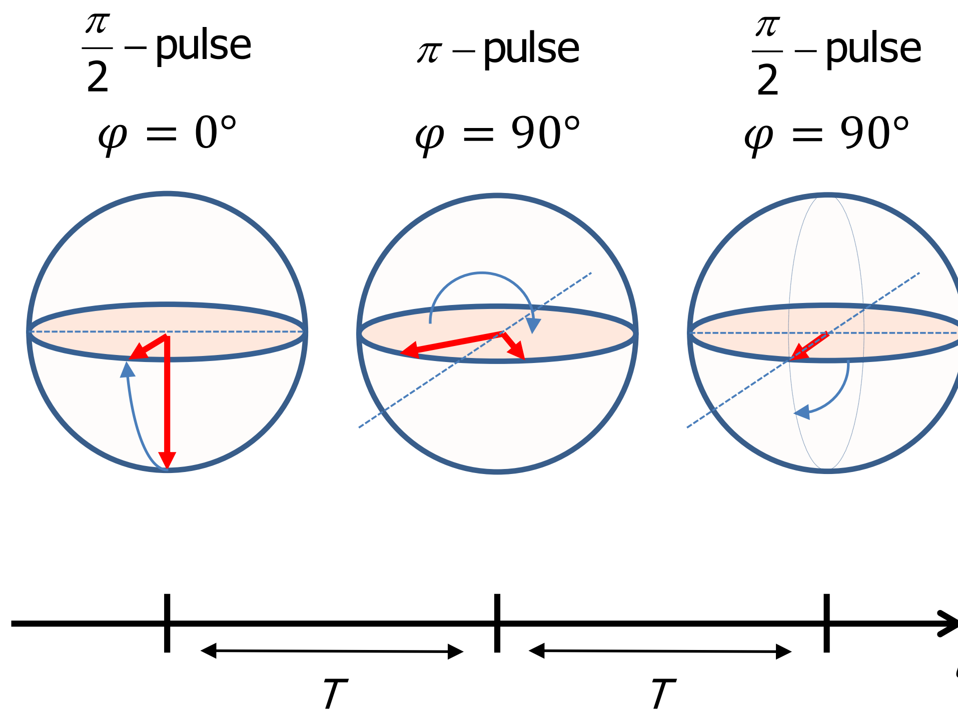

Single Clock Sagnac Effect

The University of Nottingham

Move atoms around half loop

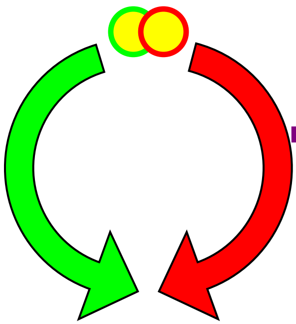

Microwave field – Ramsey Sequence
removes dynamic clock phase
acquires Sagnac phase

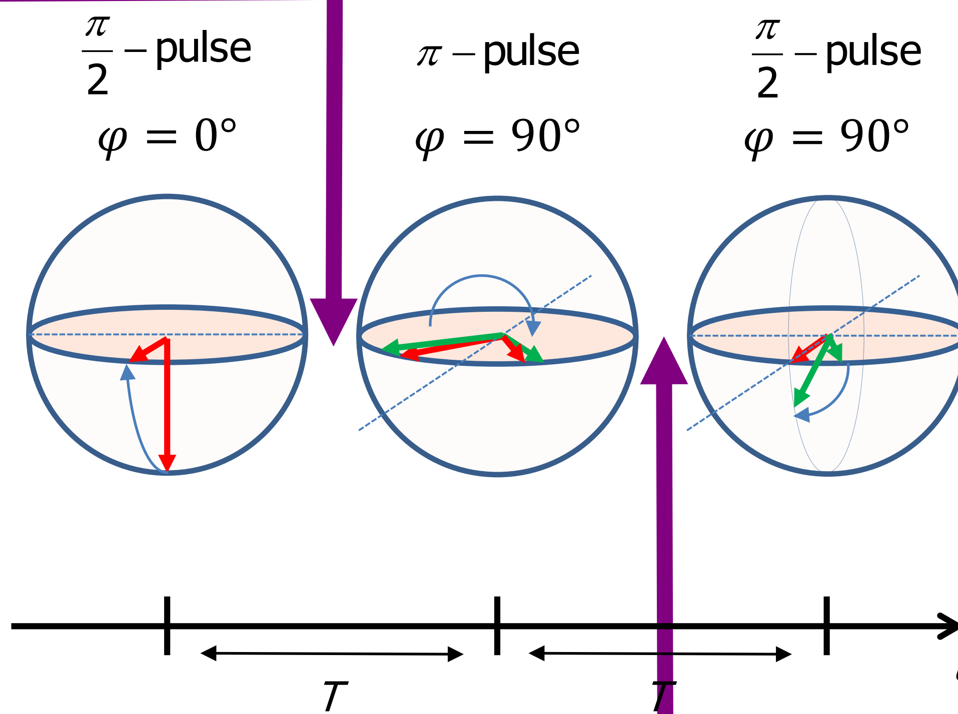

swap states,
reverse direction!

Move atoms to <u>complete loop</u>

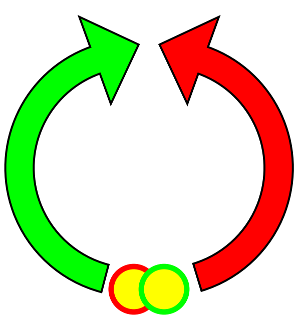

Expectation for Transported Traps

1D "harmonic" traps on ring (banana-shaped)

Measured population difference:

$$\langle \hat{\sigma}_z \rangle = C_{1D} \cos\left(\frac{m}{\hbar} 2\pi \, R^2 \Omega \right)$$

Reduced contrast due to reduced final state overlap (white light interferometer for finite temperature θ:

$$C_{1D} = e^{-|\Delta\alpha|^2 \left(\frac{1}{2} + \frac{k_B \theta}{\hbar\omega} \right)}$$

R. Stevenson et al., PRL **115**, 163001 (2015), arXiv:1504.05530

2D Isotropic Traps

Radial motion must be considered:

- Enclosed area depends on dynamics (centrifugal forces)
- For non zero rotation, centrifugal forces depend on path
- Interferometer contrast depends on rotation

Scale factor for flat-top drive profile

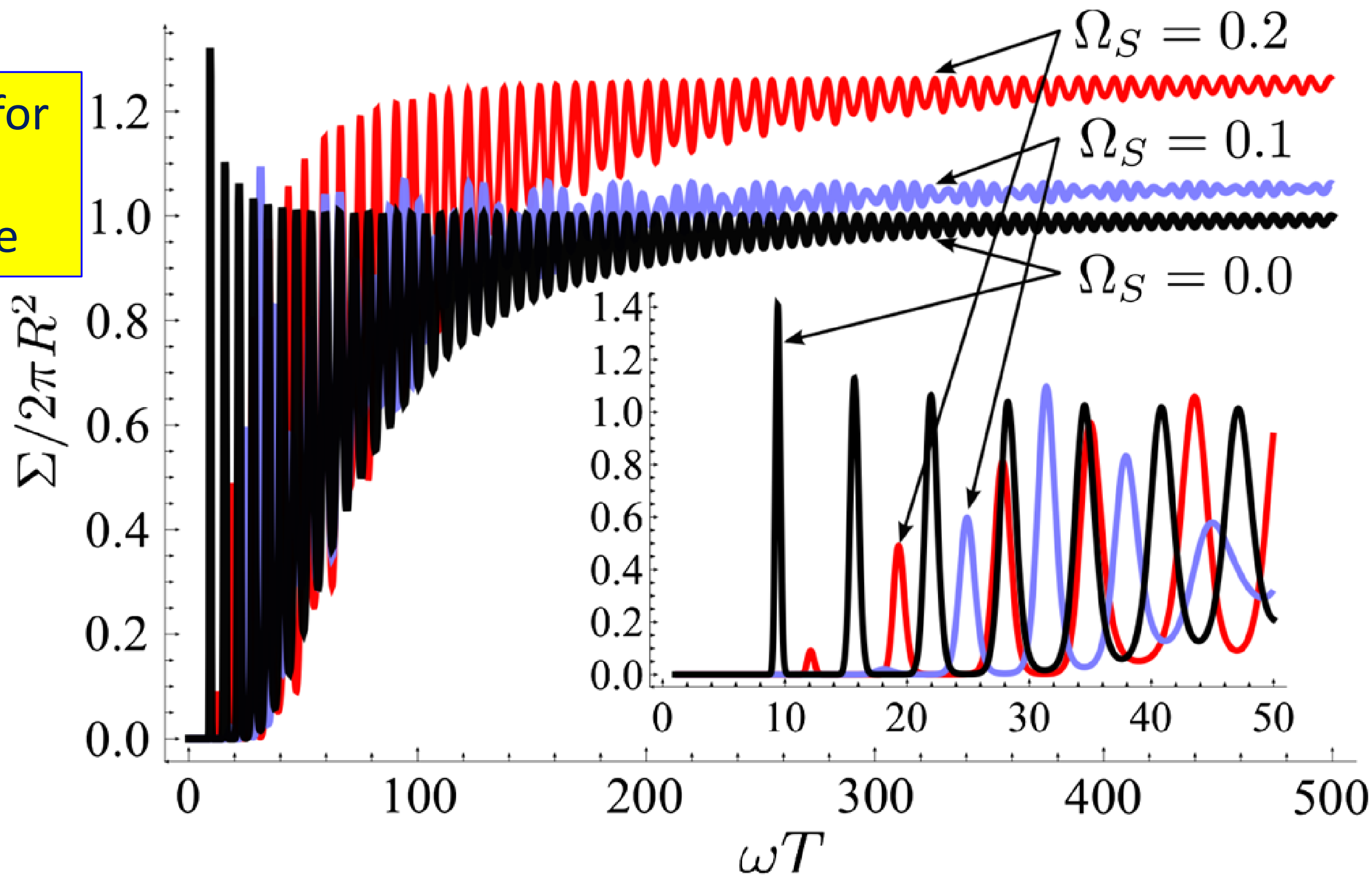

R. Stevenson et al., PRL **115**, 163001 (2015), arXiv:1504.05530

RF-Dressed Potentials

Spin F atom in magnetic field

$$\hat{H} = g_F \mu_B \mathbf{B}(t) \cdot \hat{\mathbf{F}}$$

In spherical coordinates,

static field + single radio-frequency (RF) field

$$\hat{H} = \frac{g_F \mu_B}{2} \left[B_{DC} \hat{F}_z + \left(\frac{1}{\sqrt{2}} B_+ \hat{F}_+ + \frac{1}{\sqrt{2}} B_- \hat{F}_- + B_\pi \hat{F}_z \right) e^{i\omega t} \right] + c.c.$$

Rotating frame transformation

$$\hat{H}_{\mathrm{rot}} = \frac{g_F \mu_B}{2} \left[\left(B_{DC} - \frac{\hbar\omega}{g_F \mu_B} \right) \hat{F}_z + \frac{1}{\sqrt{2}} B_+ \hat{F}_+ + \frac{1}{\sqrt{2}} B_+ \hat{F}_- e^{2i\omega t} + B_\pi \hat{F}_z e^{i\omega t} \right] + c.c.$$

Rotating wave approximation

$$\hat{H}_{\mathrm{RWA}} = \frac{g_F \mu_B}{2} \left[\left(B_{DC} - \frac{\hbar\omega}{g_F \mu_B} \right) \hat{F}_z + \frac{1}{\sqrt{2}} B_+ \hat{F}_+ \right] + c.c.$$

$$= g_F \mu_B \mathbf{B}_{\mathrm{eff}} \cdot \hat{\mathbf{F}}$$

Adiabatic RF Dressing

laboratory frame

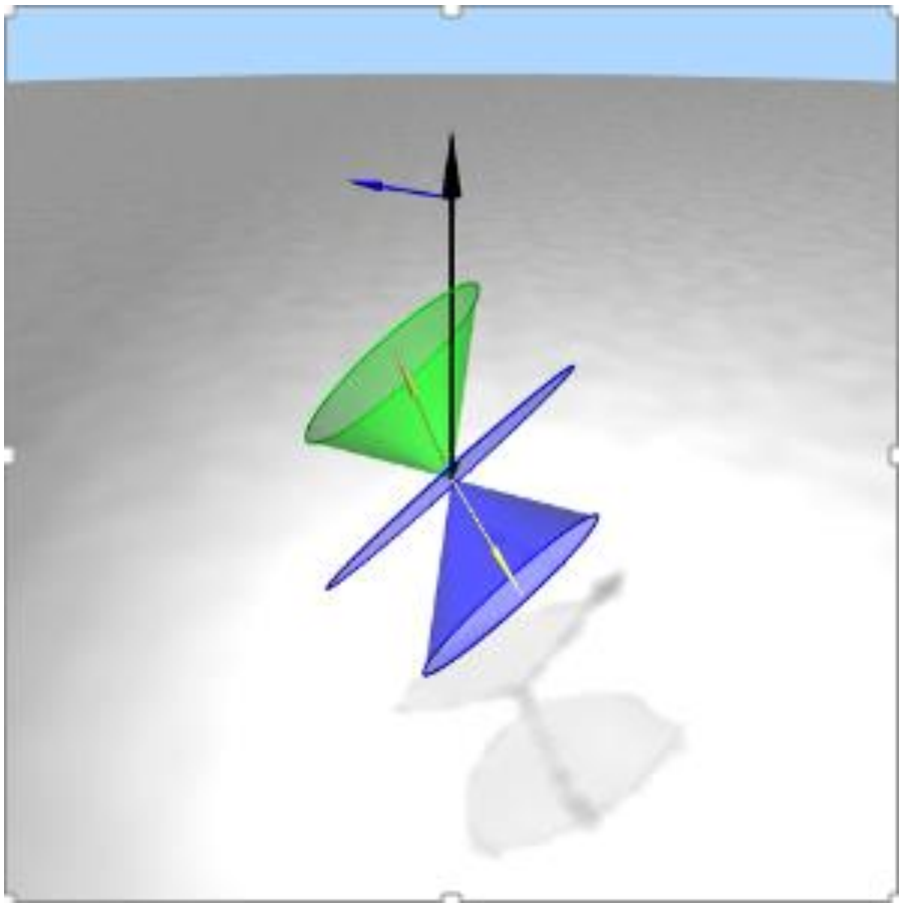

rotating frame

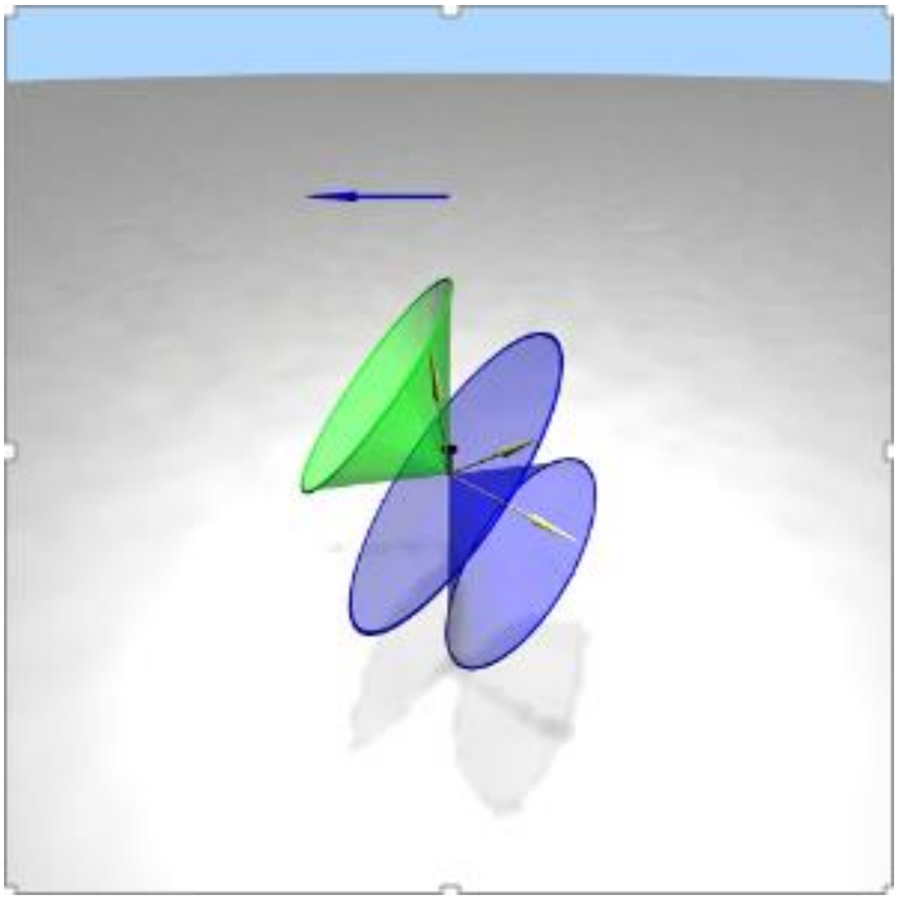

RF-Dressed Potentials

Atoms in static field gradient with RF coupling

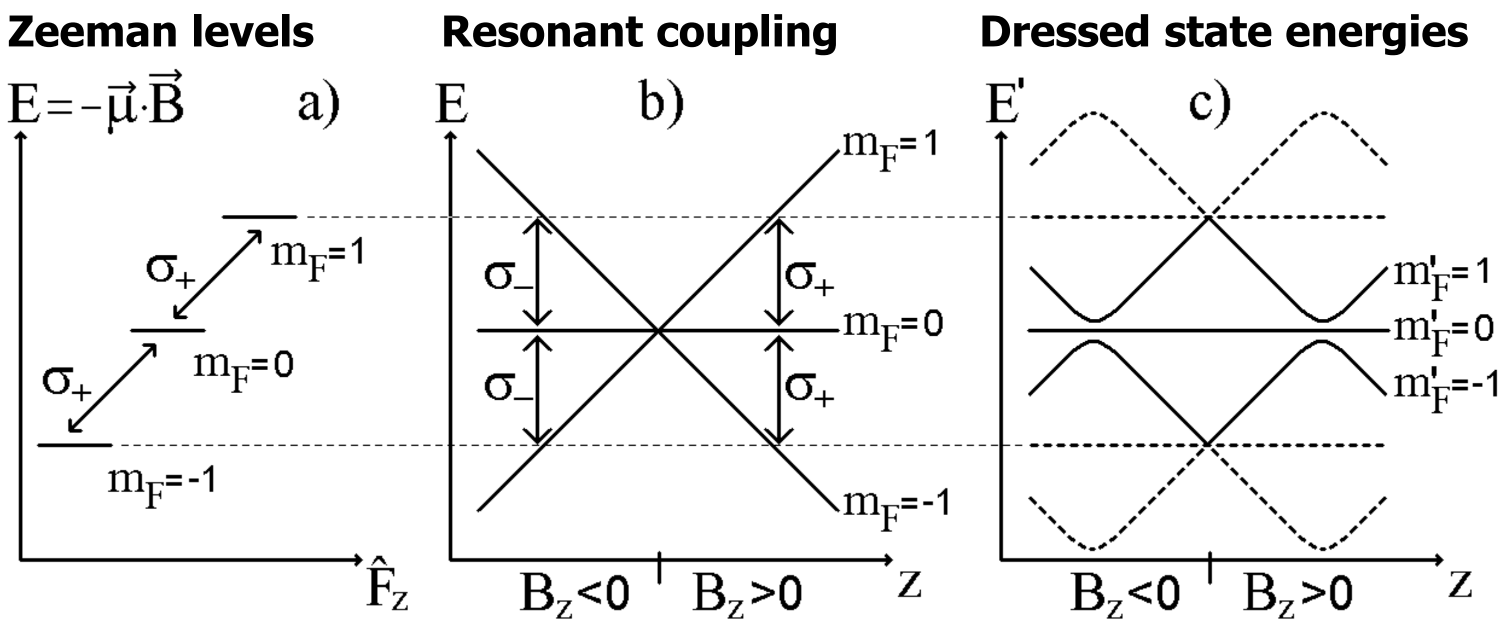

Adiabatic potential in RWA (given by effective field strength)

$$U(z) = m'_F g_F \mu_B \sqrt{\left(B_{DC} - \frac{\hbar\omega}{g_F \mu_B}\right) + \frac{1}{2}|B_+|^2}$$

minimal at resonant field magnitude

Resonant Potential - Polarization

Within resonant manifold, potential is determined by

local σ_+ component: $B_+ = \mathbf{e}_+ \cdot \mathbf{B}_{\mathrm{RF}}$

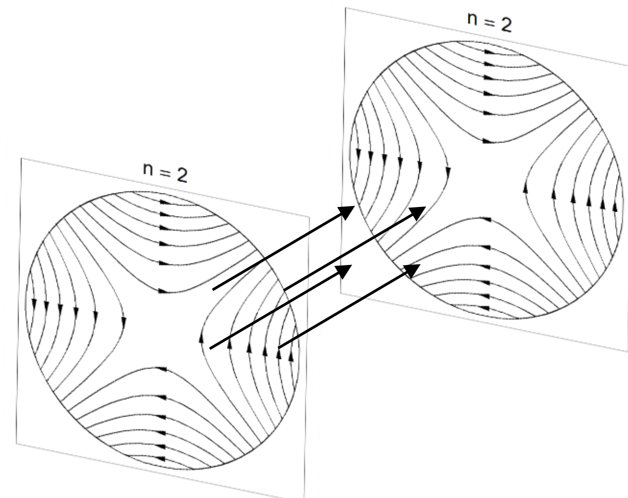

Example: Ioffe trap + **global**, spherical RF components

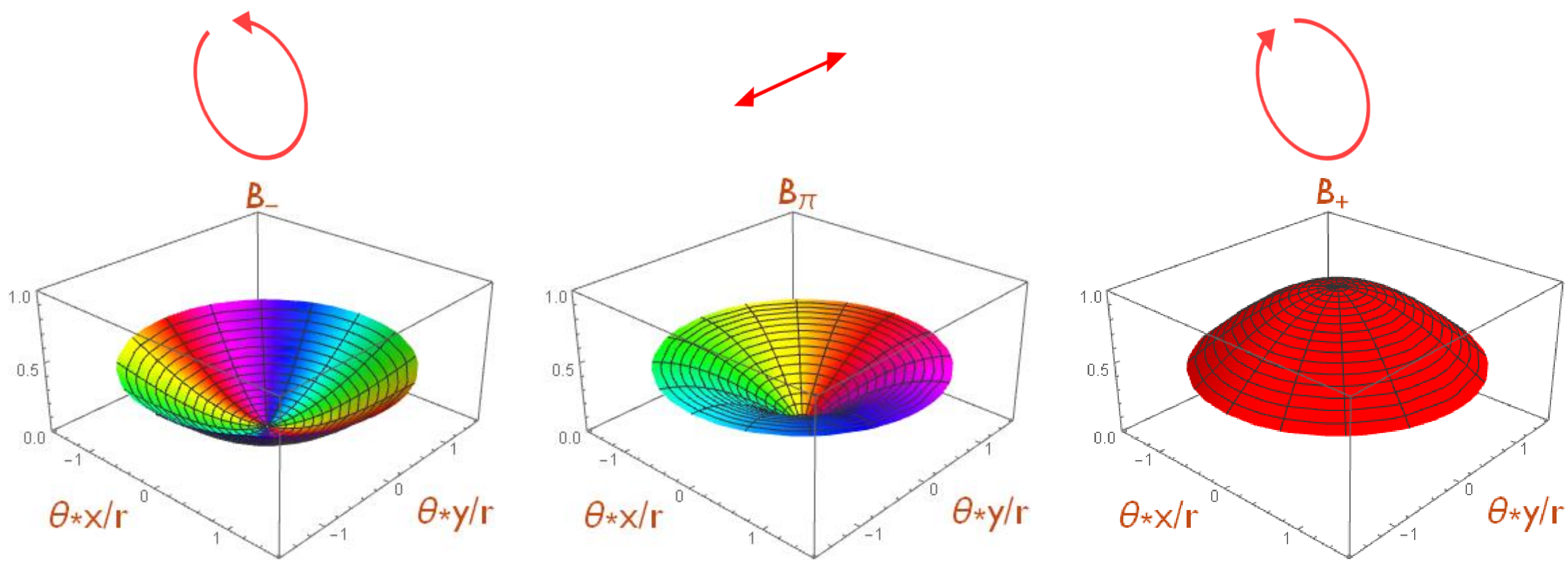

Resonant Potential - Polarization

Within resonant manifold, potential is determined by

local σ_+ component: $B_+ = \mathbf{e}_+ \cdot \mathbf{B}_{\mathrm{RF}}$

Example: Ioffe trap + global, spherical RF components

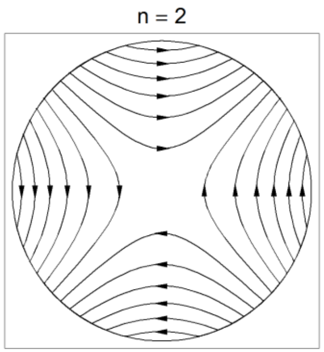

Double well potential

coupling

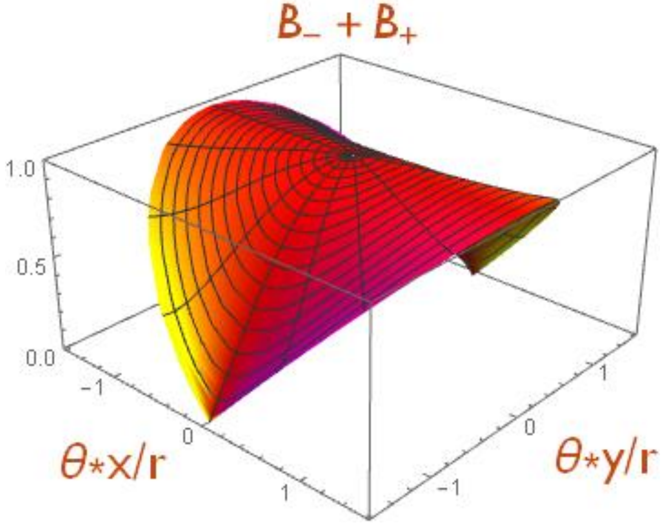

dressed potential

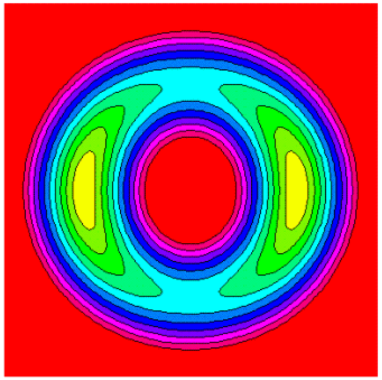

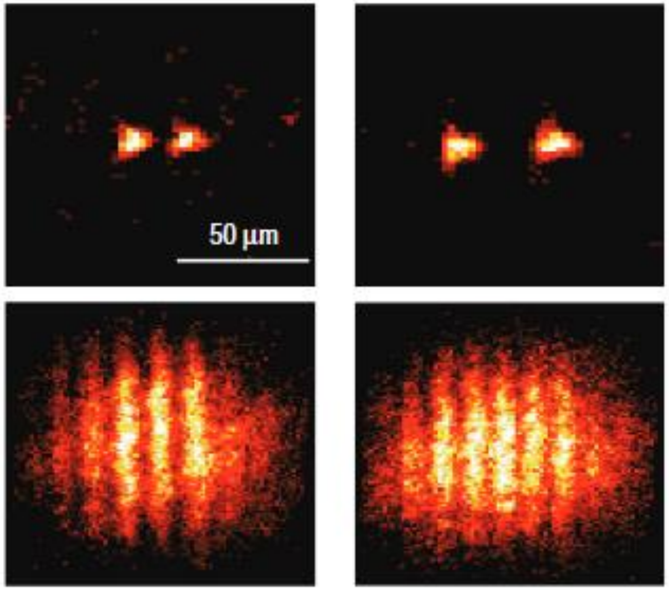

T. Schumm et al., Nat. Phys. **1**, 57 (2005)

Ring Traps

- Ring-shaped, cylindrical quadrupole field
  (use two rings of permanent magnetic material)
- RF quadrupole field + vertical field (90° phase)
  (high gradient required for small rings)

$$\mathbf{B}_{RF}(t) = \mathrm{Re}\left[\mathbf{B}_{\mathbf{a,b}} \cdot e^{-i\omega t}\right]$$

$$\mathbf{B}_{\mathbf{a,b}} \approx \frac{a}{\sqrt{2}}\begin{pmatrix}\cos\theta \\ \sin\theta \\ +i\end{pmatrix} + \frac{b}{\sqrt{2}}\begin{pmatrix}\cos\theta \\ \sin\theta \\ -i\end{pmatrix}$$

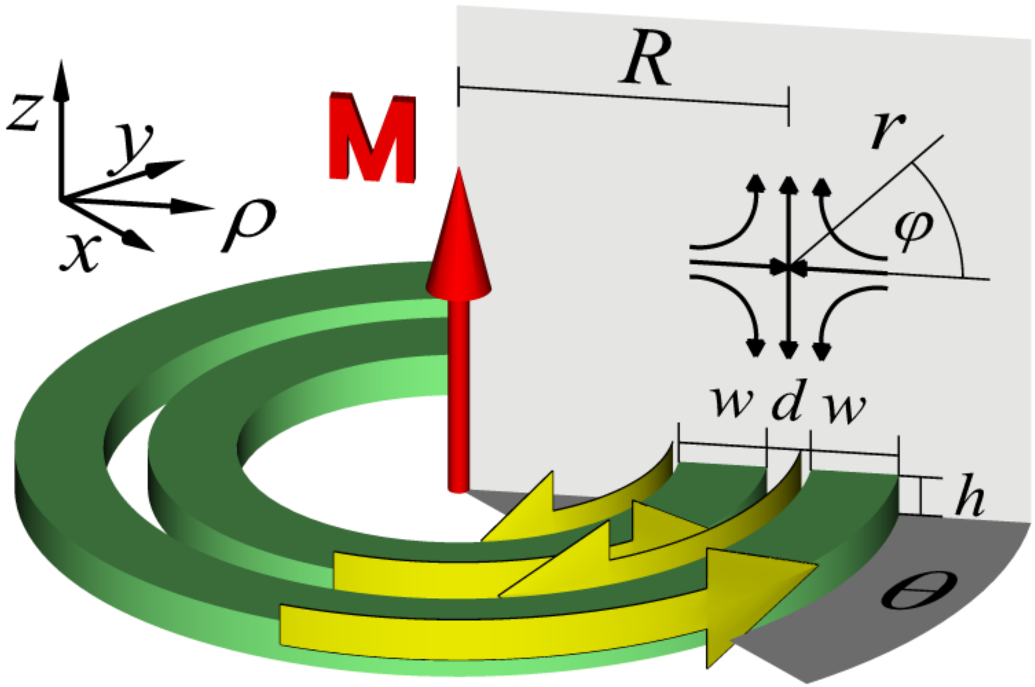

+

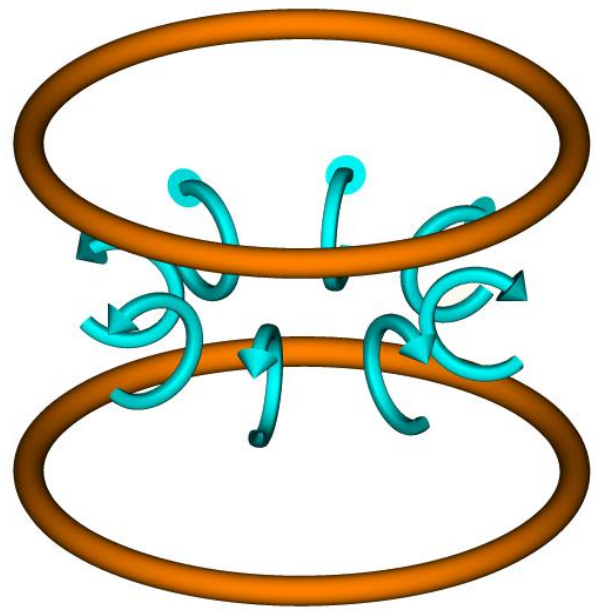

T. Fernholz et al., "Toroidal and ring-shaped traps with control of atomic motion", PRA **75**, 063406 (2007).

Resulting Potentials

Potential on the resonant torus

(given by local coupling strength $|B_+|$)

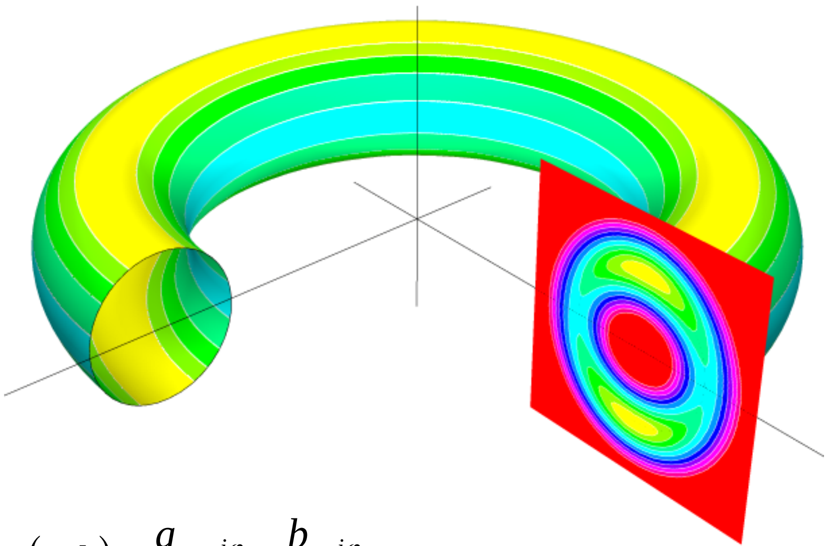

$$B_+(a,b) = \frac{a}{2}e^{-i\varphi} - \frac{b}{2}e^{i\varphi}$$

$$U_{m'_F} = \frac{m'_F g_F \mu_B}{2\sqrt{2}} \sqrt{|a|^2 + |b|^2 - 2|a||b|\cos\left(2\varphi - \arg\frac{a}{b}\right) + \left(\beta r - \frac{\hbar\omega}{g_F \mu_B}\right)^2}$$

r, φ -planes

circular rf
(b=0)

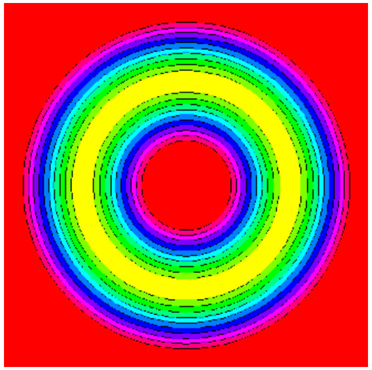

elliptical rf
(|a|>|b|>0)

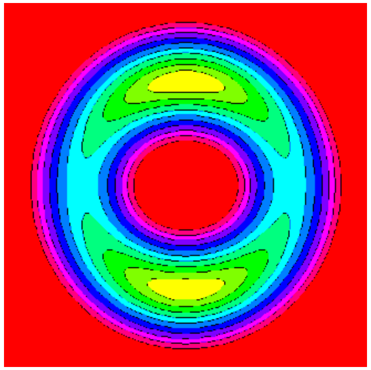

Motion Control

Atomic motion can be controlled using **only** global rf fields

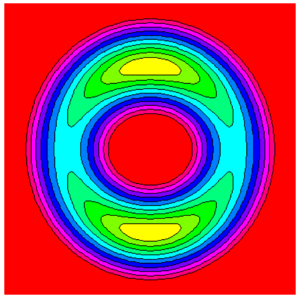

Poloidal rotation

- Induce rings using elliptical rf
- Vary relative phase between *a* and *b*.

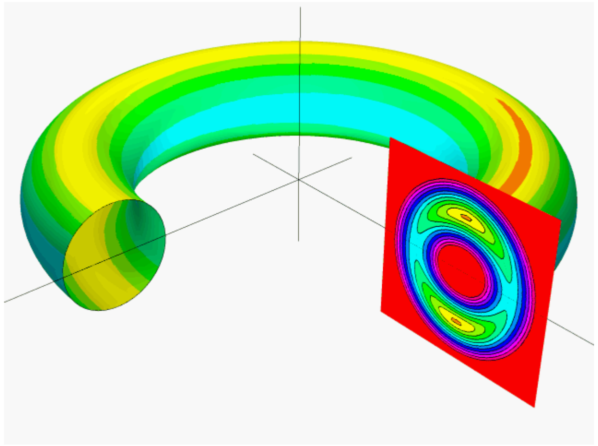

Toroidal rotation (state dependent)

- Additional in-plane (*x,y*) circular fields interfere with $\mathbf{B}_{a,b}$

Counter-propagating rings

- Create two vertically split rings
  (rf quadrupole component (ρ) > vertical component (z))
- Add in-plane (*x,y*), linearly polarized rf field
  (slightly different frequency)

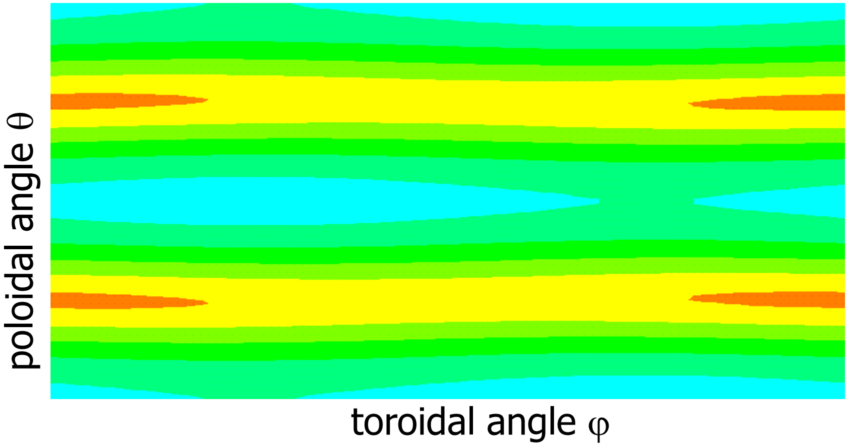

With rf fields in *x*- and *y*- directions,
the two rings or
different internal states with different
***g*-factors** can be controlled independently !

Magnetically Guided Clock

Energy of ^{87}Rubidium in B-field

$$U \approx E_{HFS} + m_J g_J \mu_B B_z$$

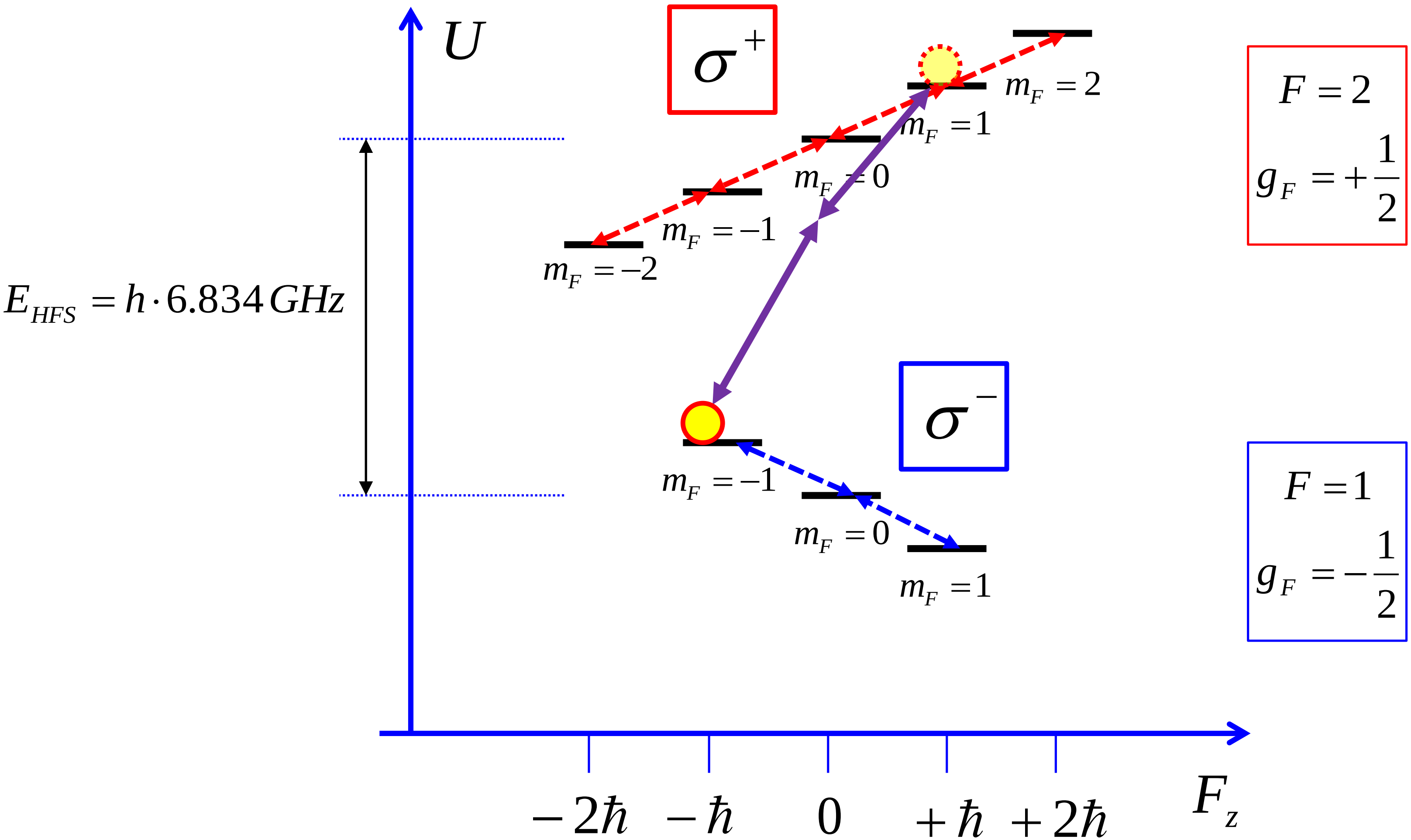

Experimental Efforts

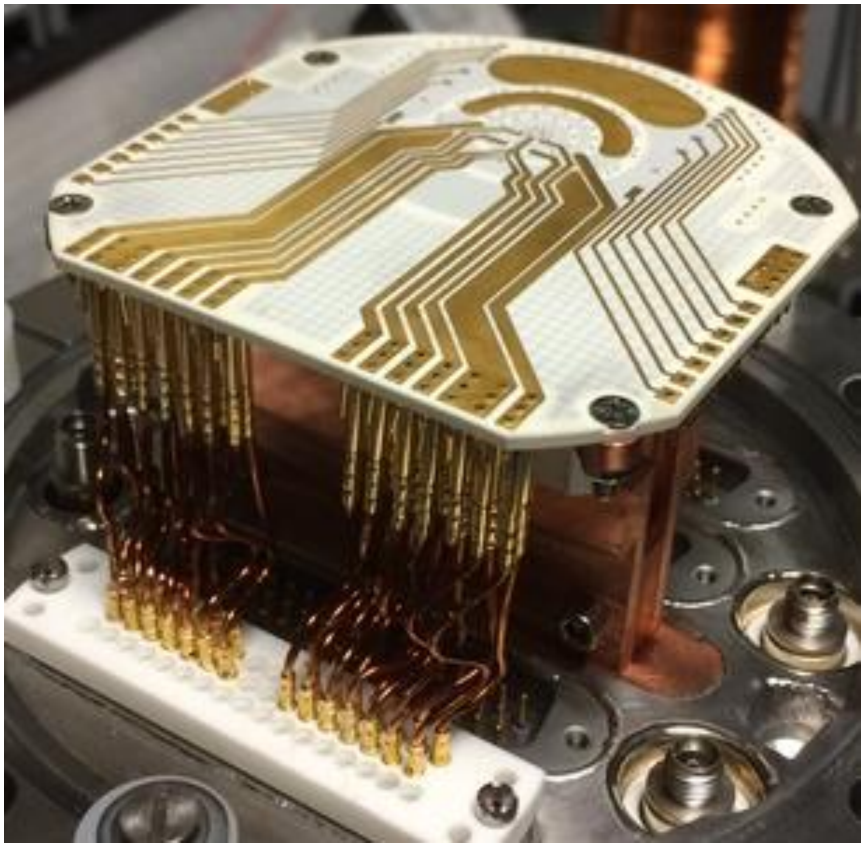

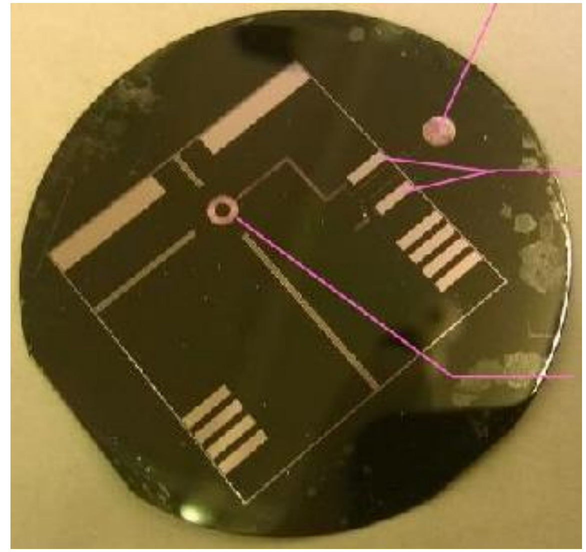

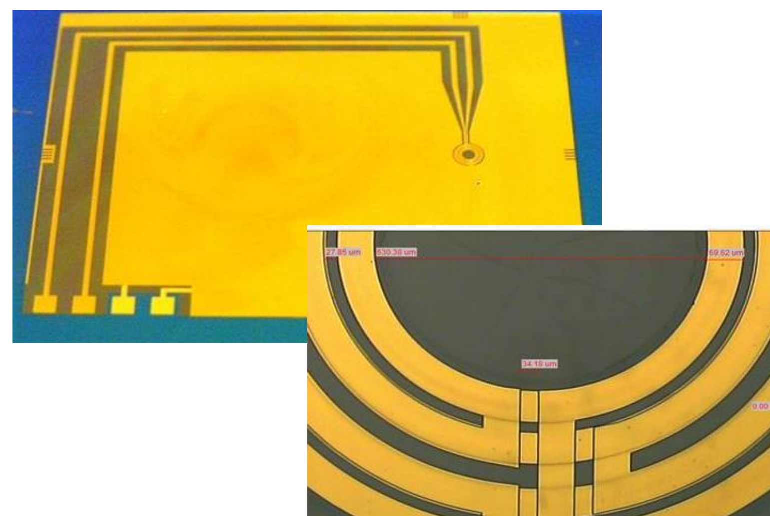

State-Dependent Guiding

See Wolf von Klitzing, Thursday 9:00

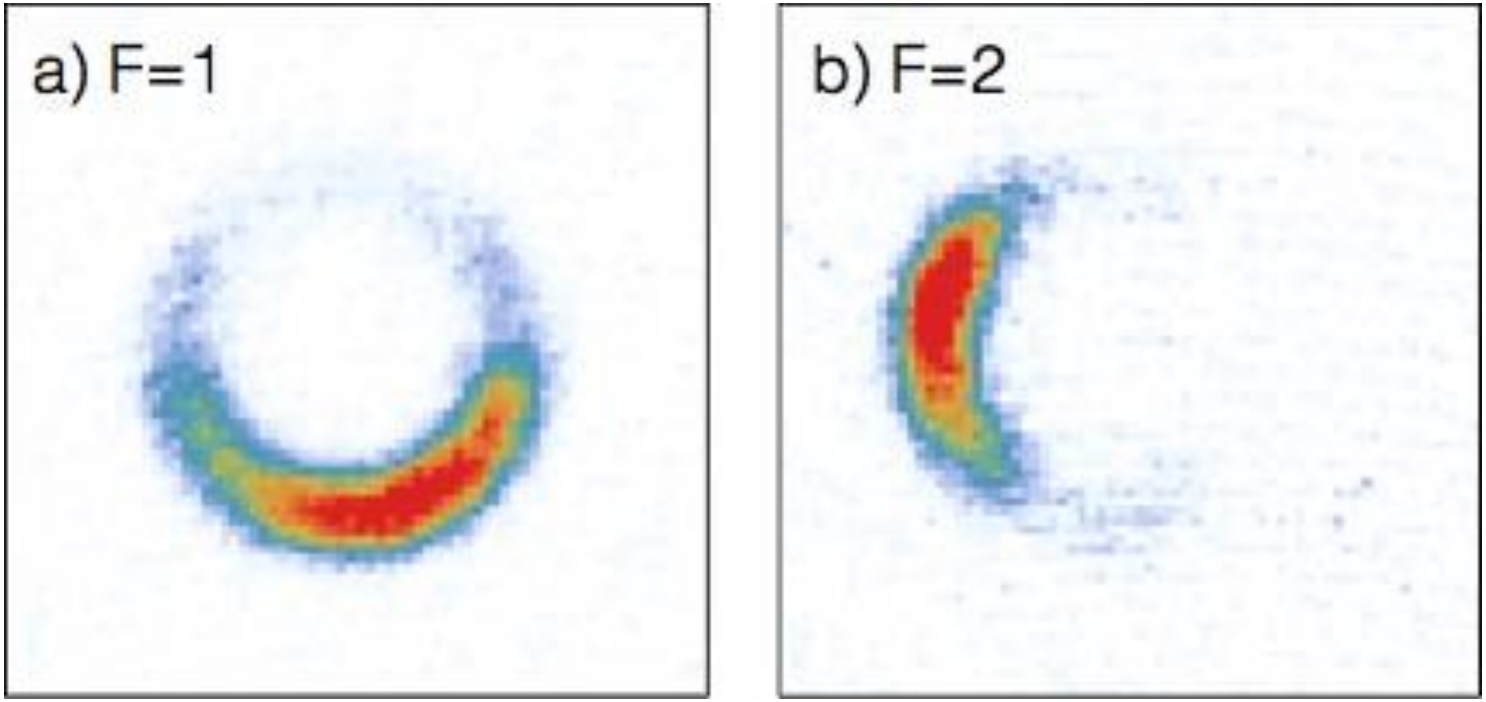

Voigt Spectroscopy

Non-destructive measurement
of linear birefringence
proportional to tensor polarizability

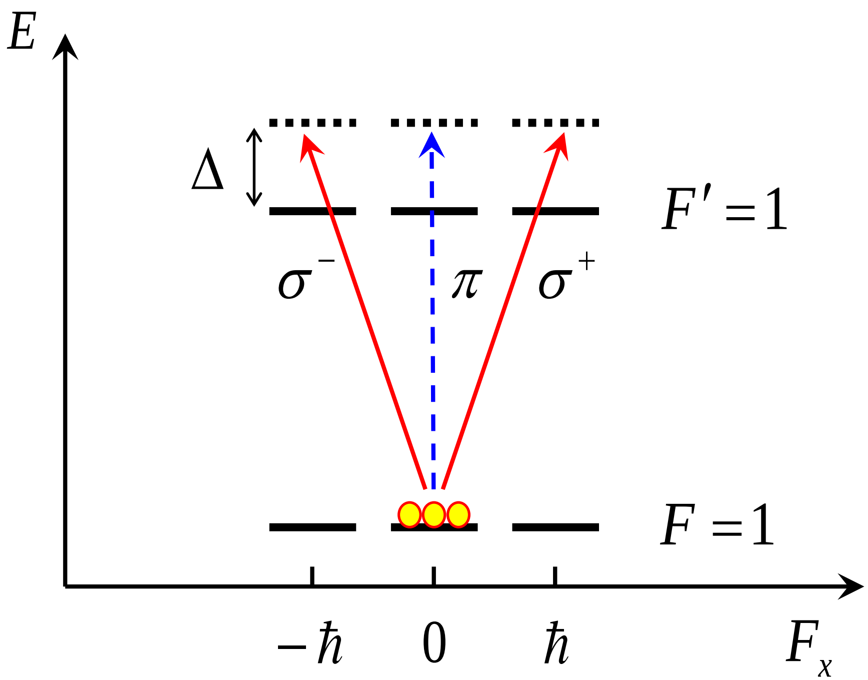

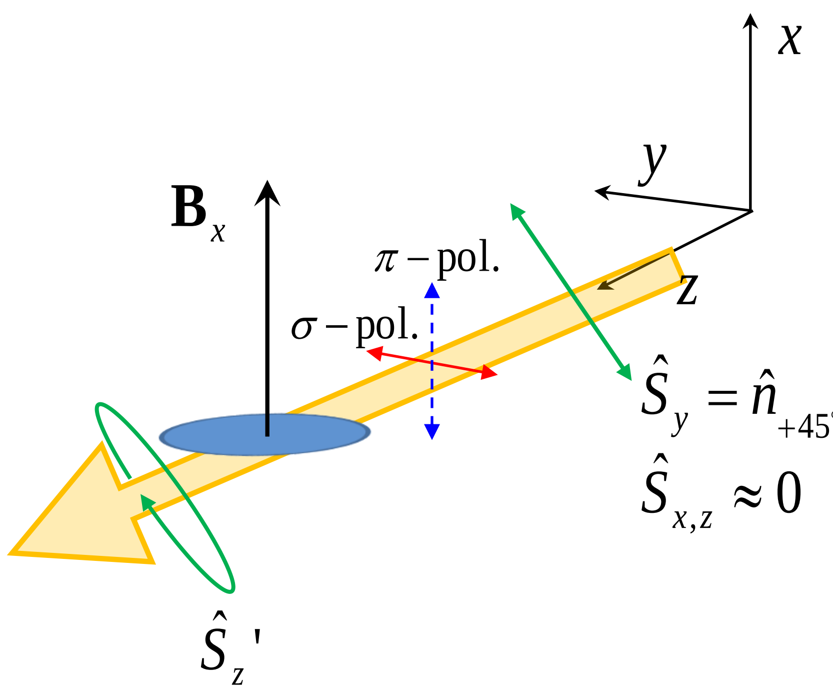

Resulting Ellipticity

Output for classical input light with 45°-polarization

$$\left(\hat{S}_z \approx 0, \quad \hat{S}_x \approx 0, \quad \hat{S}_y \approx S_y\right)$$

$$\hat{S}_z' = \hat{S}_z + \frac{\omega}{2\varepsilon_0 c}\alpha_F^{(2)} S_y \times \int \left(\hat{f}_x^2 - \hat{f}_y^2\right)\rho\, dz$$

$$\overbrace{\langle \cdots \rangle = \frac{N}{2A}\left(F(F+1) - 3m^2\right)}$$

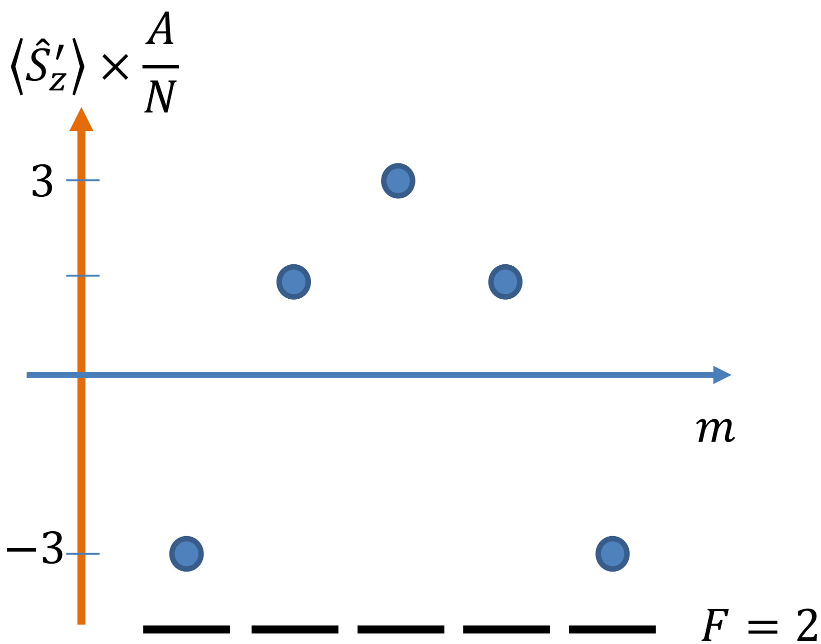

for Eigenstates of $\hat{F}_y$

$$\hat{F}_y |F, m\rangle = m\hbar |F, m\rangle$$

RF-Dressed |1,0> State

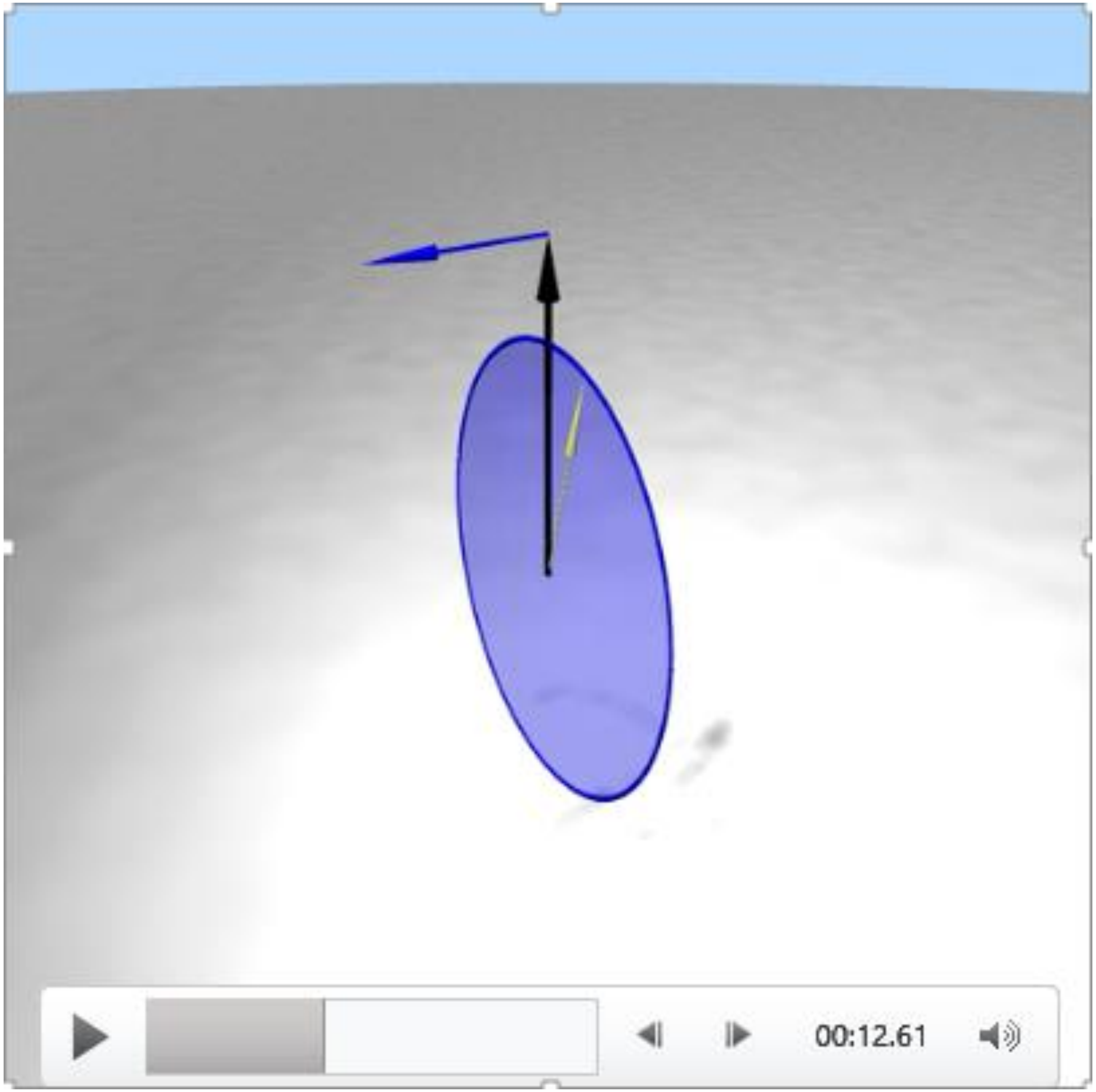

Dressed State Detection

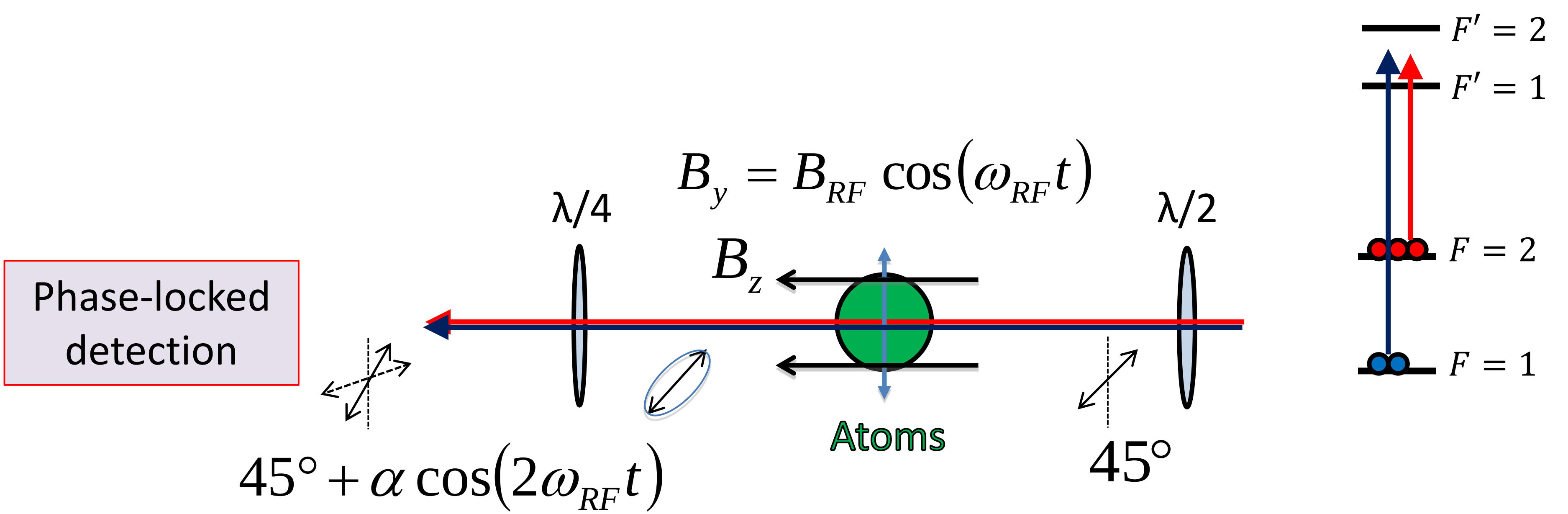

RF dressing:

$$F_z = m \quad \rightarrow \quad F_x \cos(\omega_{RF} t) + F_y \sin(\omega_{RF} t) = m$$

Dressed Probing of Bare Clock

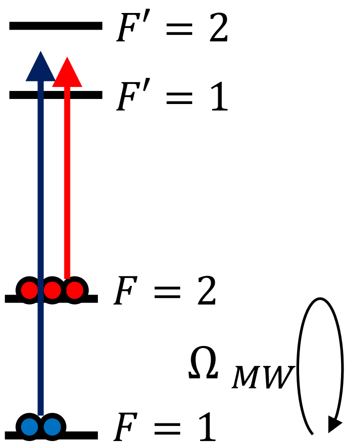

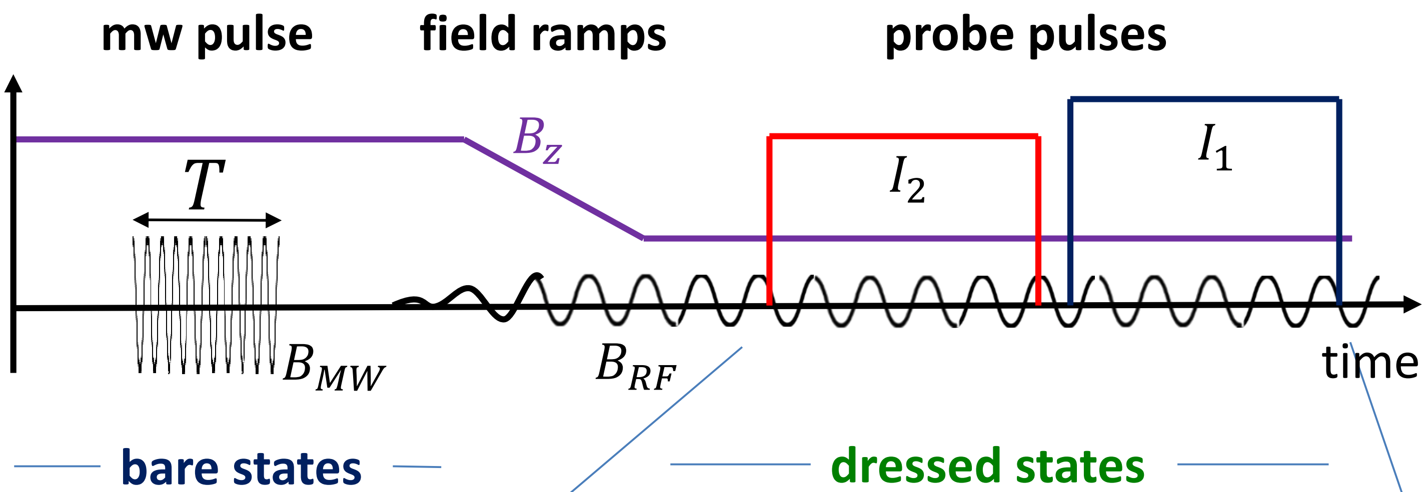

Standard clock transition

$|1,0\rangle \rightarrow |2,0\rangle$

(starting from pure state)

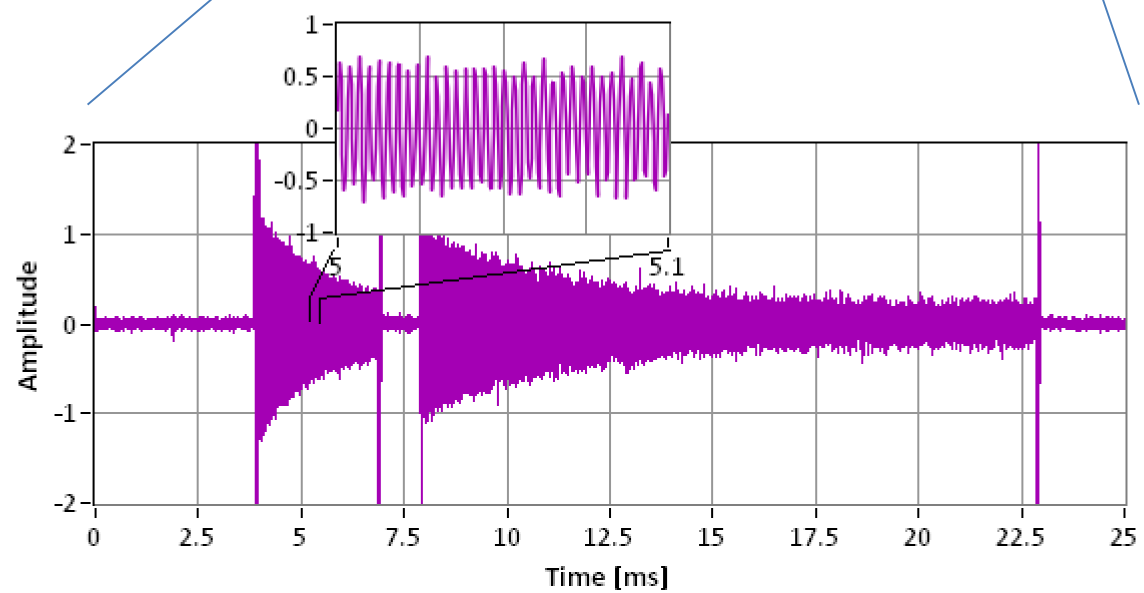

Bare Clock Rabi Cycles

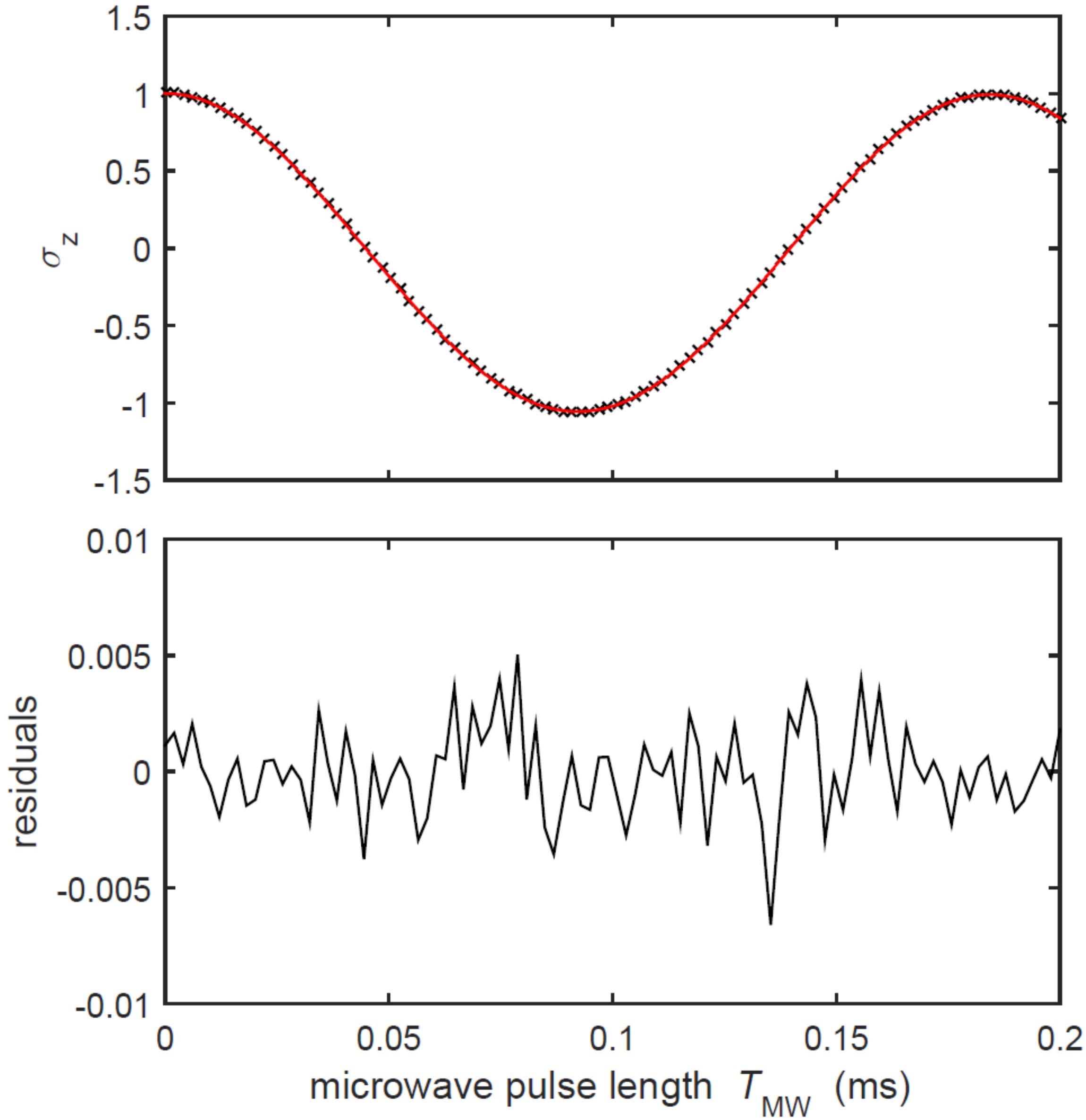

Dressed Clock?

The University of Nottingham

Energy of [87]Rubidium in B-field

$$U \approx E_{HFS} + m_J g_J \mu_B B_z$$

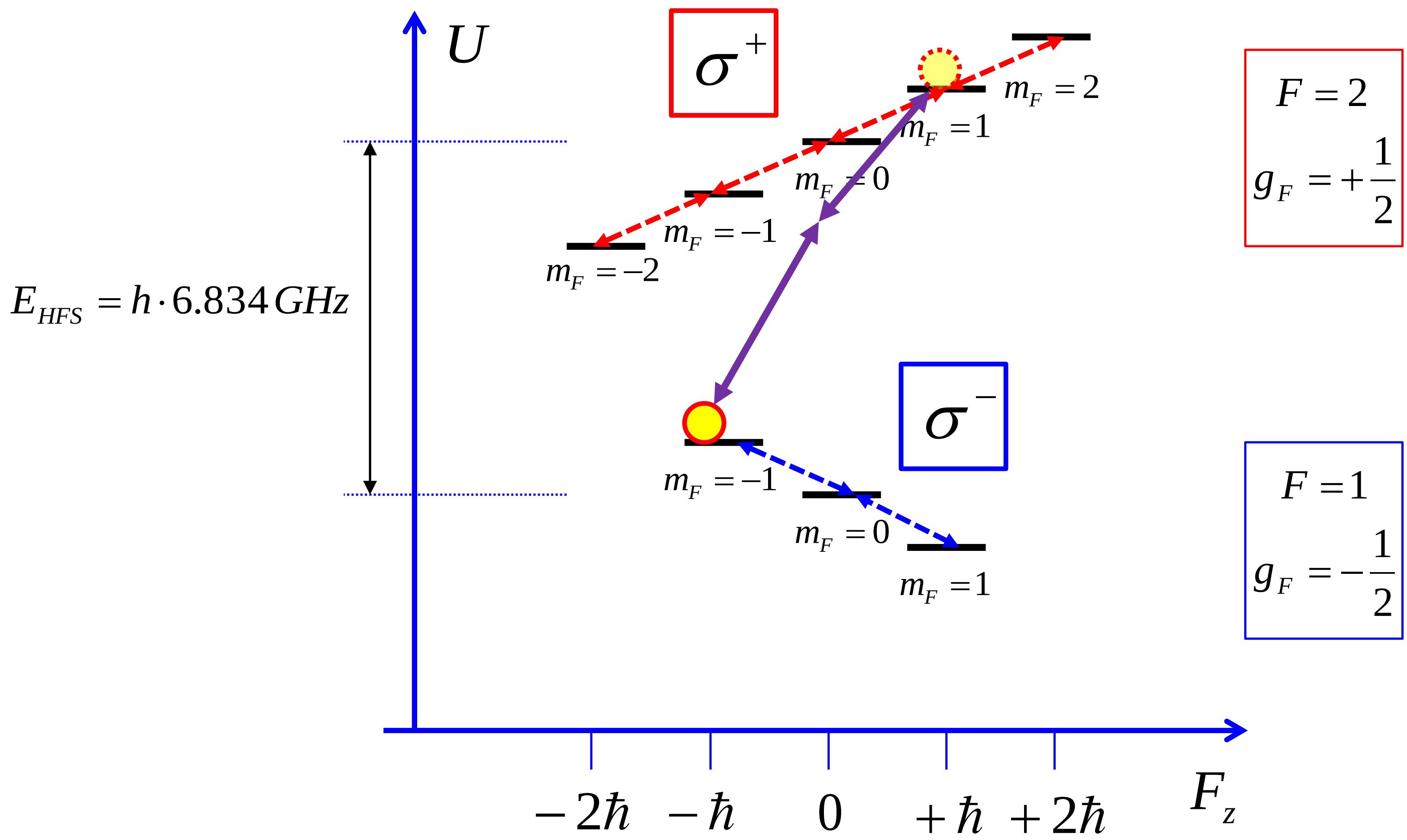

Dressed MW transitions

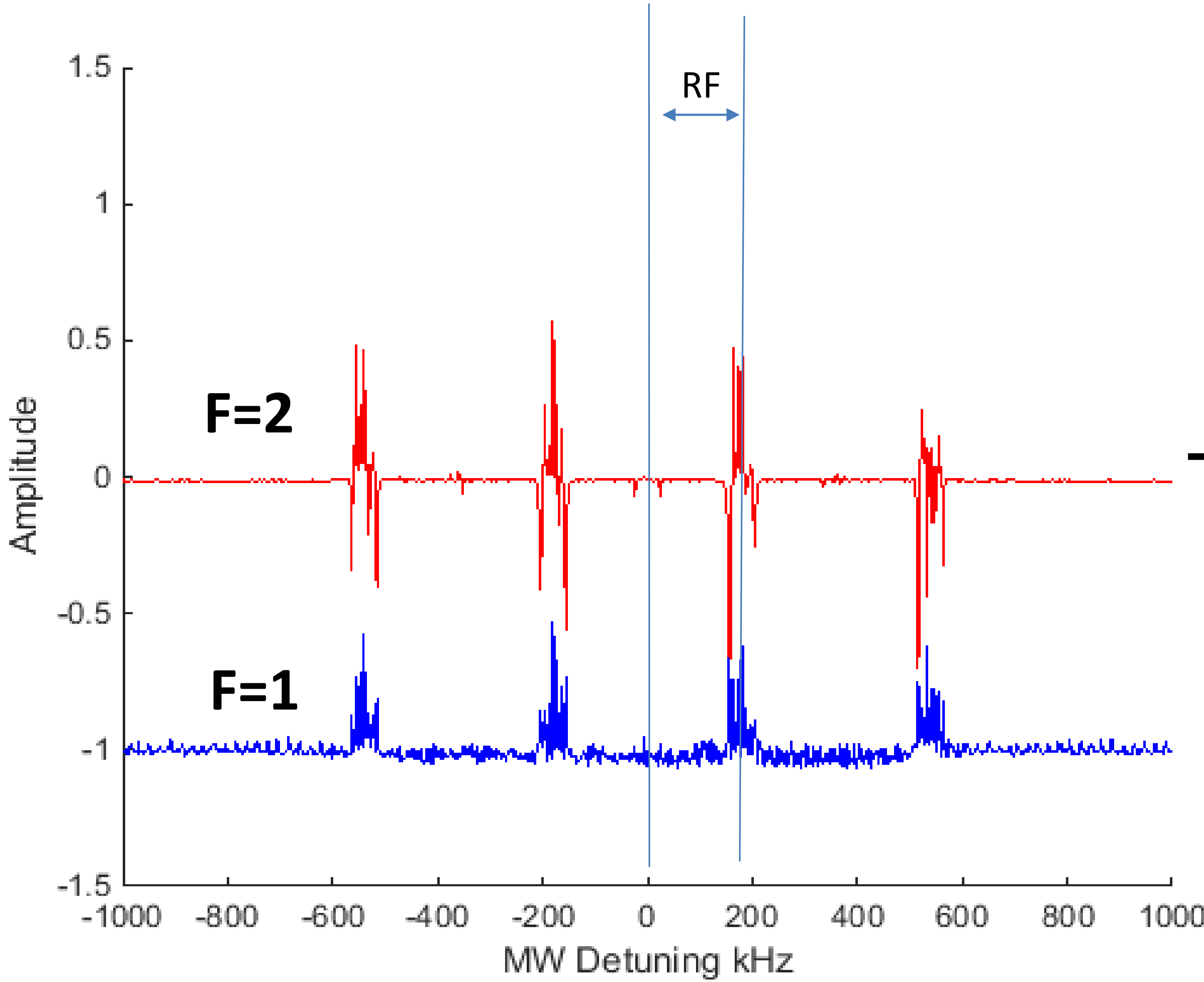

from bare clock transition (6.834 GHz)

Linear RF & MW, all fields orthogonal

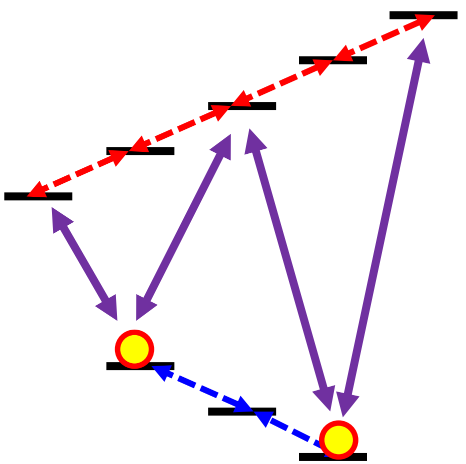

Initial states |1,-1> & |1,+1> populated

Dressed MW transitions

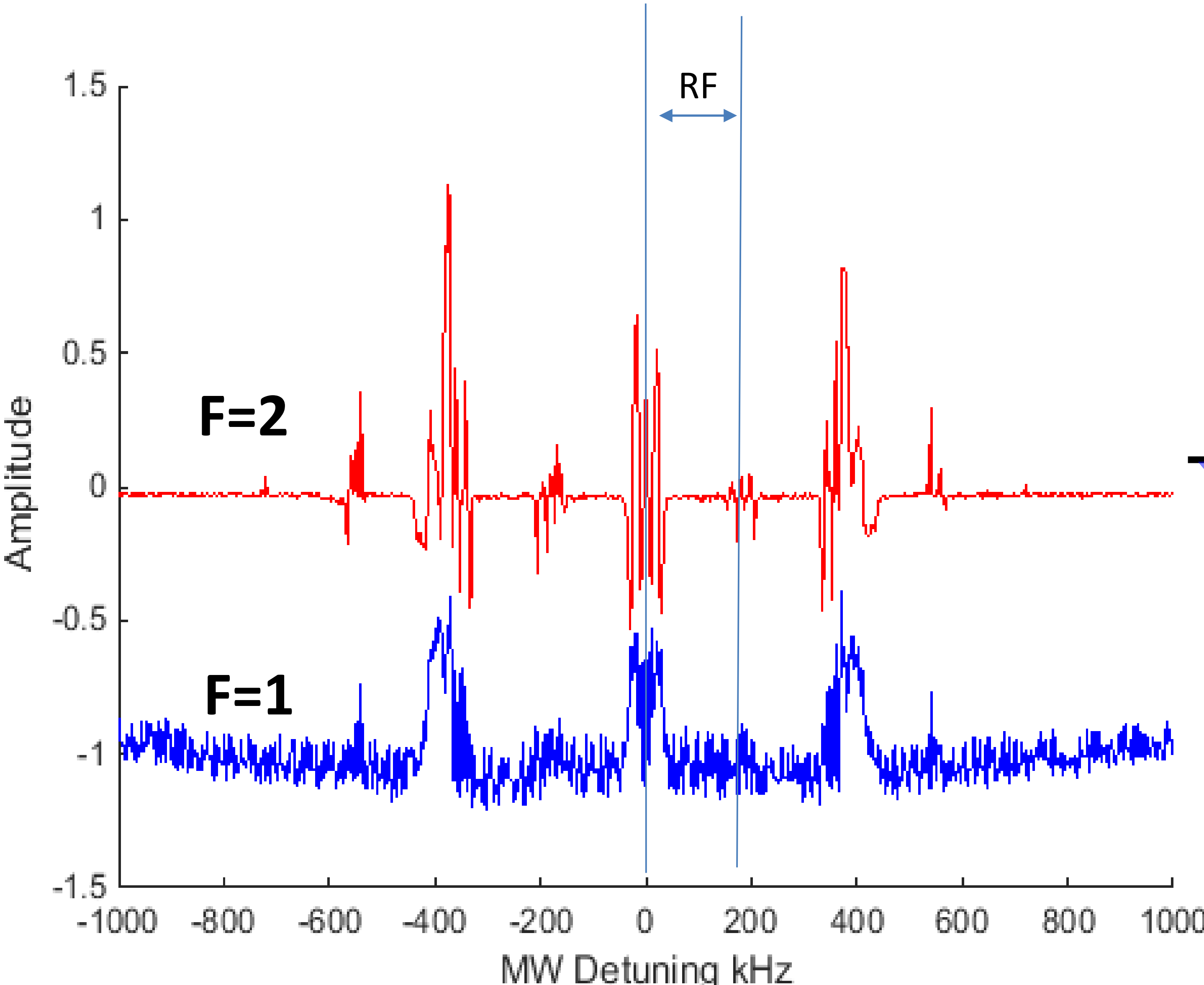

from bare clock transition (6.834 GHz)

MW field & static field parallel

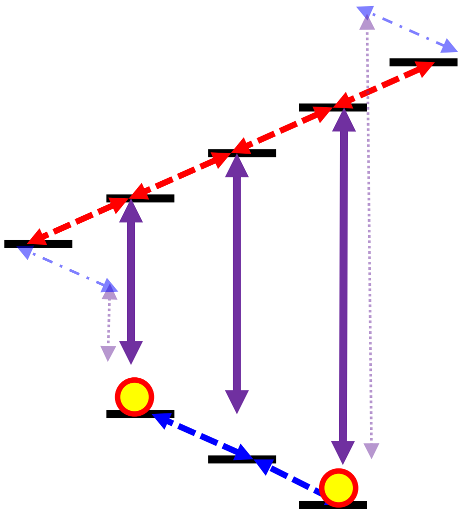

Initial states |1,-1> & |1,+1> populated

Coupling of Dressed States

atom
+ static field
+ RF field

microwave
coupling

$$\hat{H} = \hat{H}_0(t) + \hat{H}_1 \cos(\omega_{\mathrm{MW}} t)$$

Hamiltonian expanded in dressed state basis

$$\hat{H}' = i\hbar \frac{\partial}{\partial t}\hat{U}\hat{U}^\dagger + \hat{U}\hat{H}_0\hat{U}^\dagger + \hat{U}\hat{H}_1\cos(\omega_{\mathrm{MW}}t)\hat{U}^\dagger$$

$$= \sum_n E_n |\Phi_n\rangle\langle\Phi_n| + \sum_{m,n} |\Phi_m\rangle\langle\Phi_m|\hat{U}(t)\hat{H}_1\cos(\omega_{\mathrm{MW}}t)\hat{U}^\dagger(t)|\Phi_n\rangle\langle\Phi_n|$$

$$= \sum_n E_n |\Phi_n\rangle\langle\Phi_n| + \sum_{m,n} |\Phi_m\rangle\langle\Psi_m(t)|\hat{H}_1\cos(\omega_{\mathrm{MW}}t)|\Psi_n(t)\rangle\langle\Phi_n|$$

modulated coupling =

instantaneous coupling elements between lab-frame solutions

Dressed, Trappable Clock States

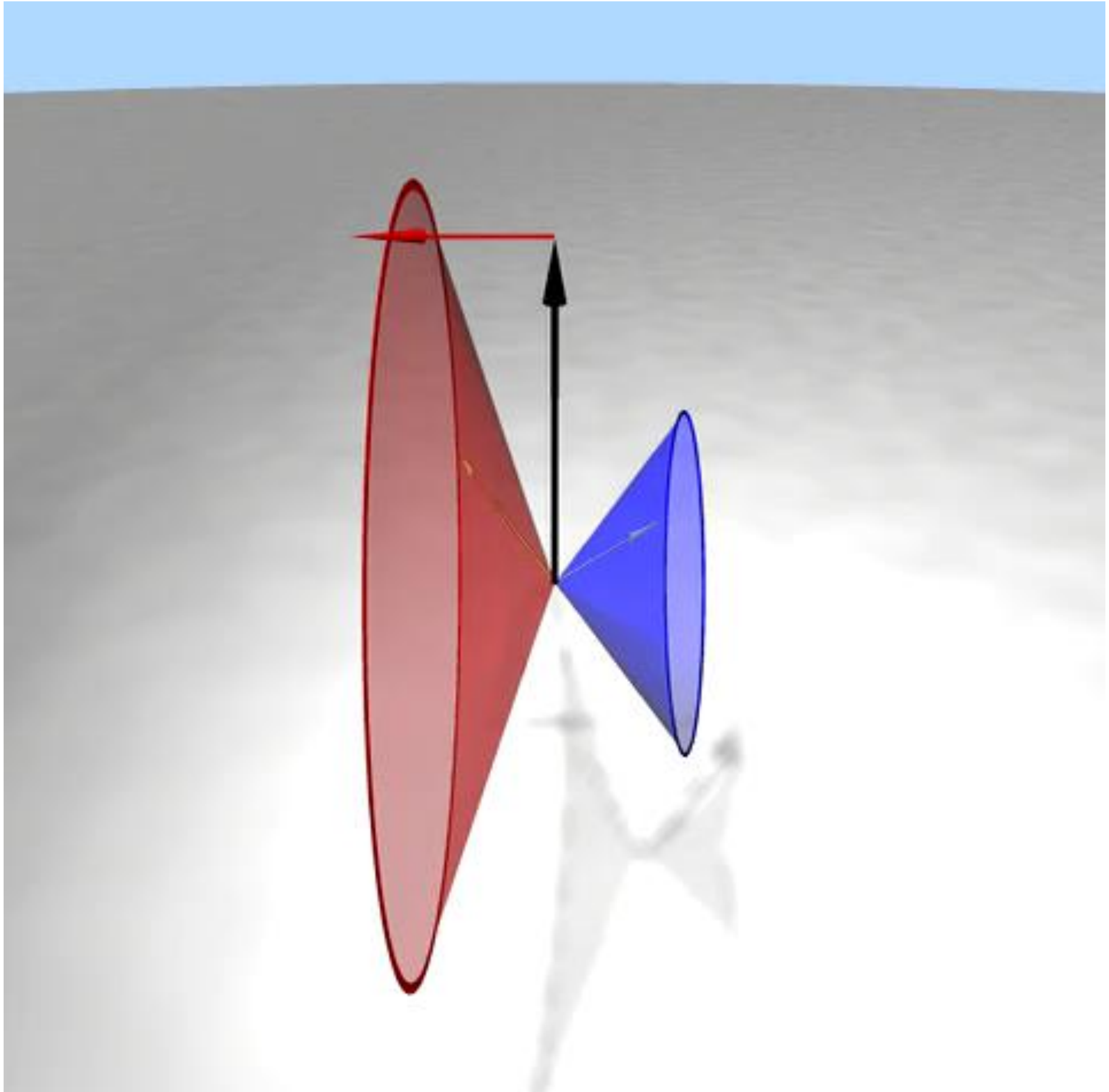

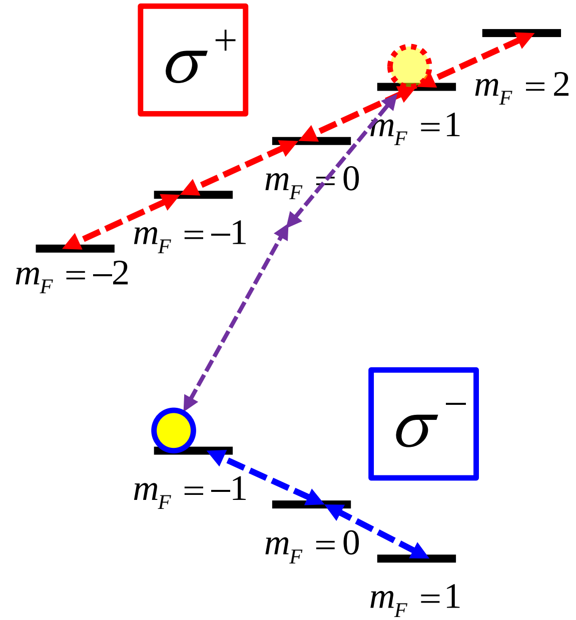

A Useful Picture

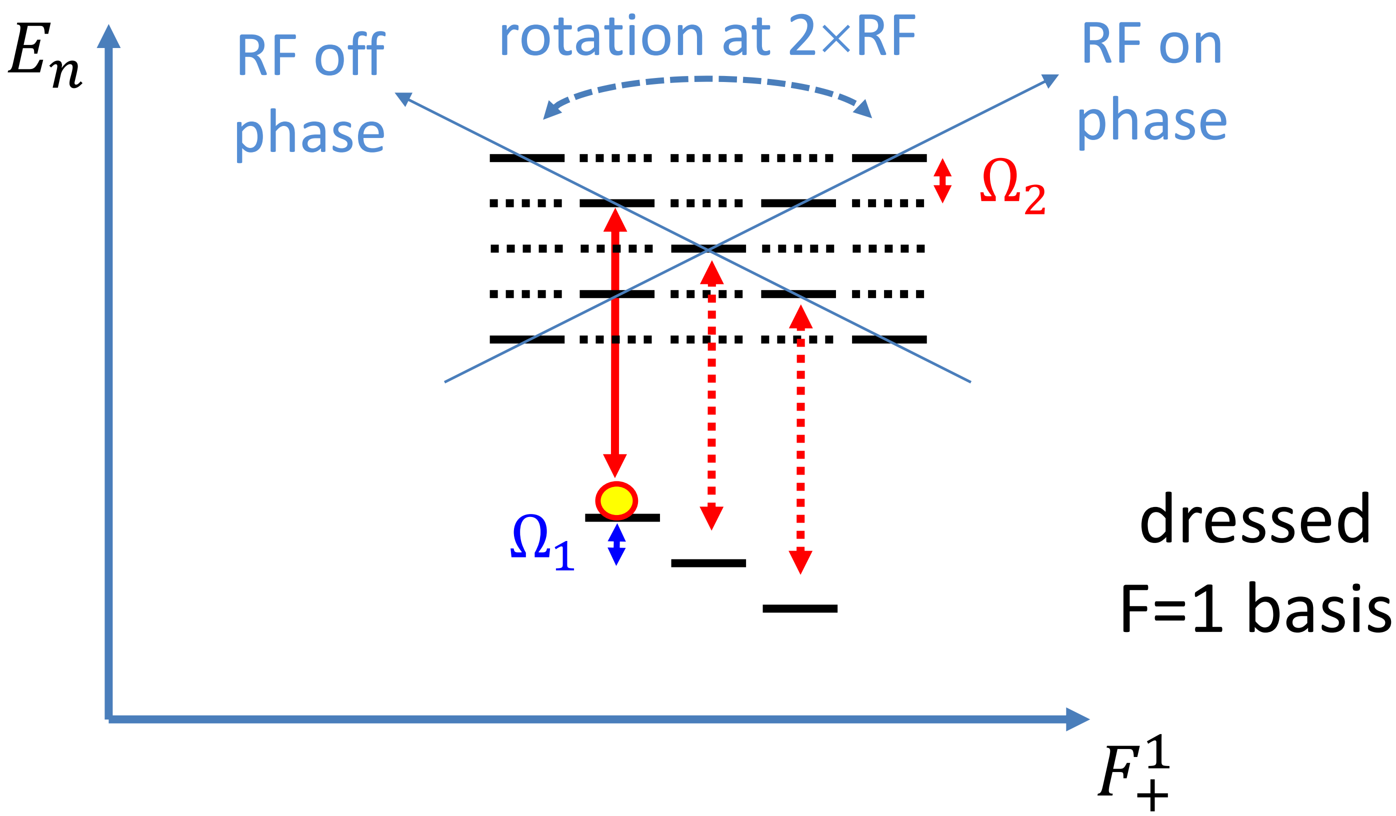

A triplet of sharp transitions is expected for all fields orthogonal, at $\pm 1\times$RF.
One transition between trappable states.

First groups ($\pm 1 \times$ RF)

All fields orthogonal

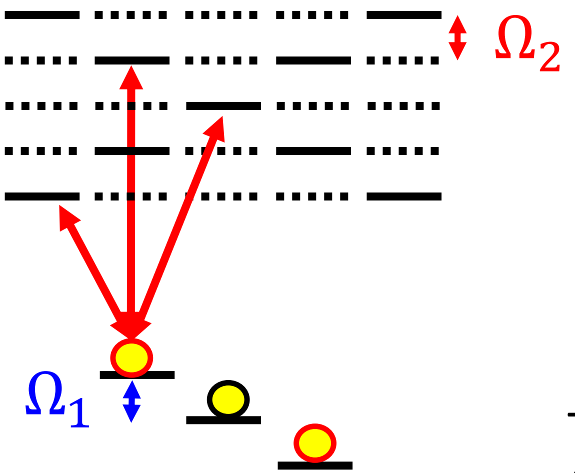

-1×RF group

+1×RF group

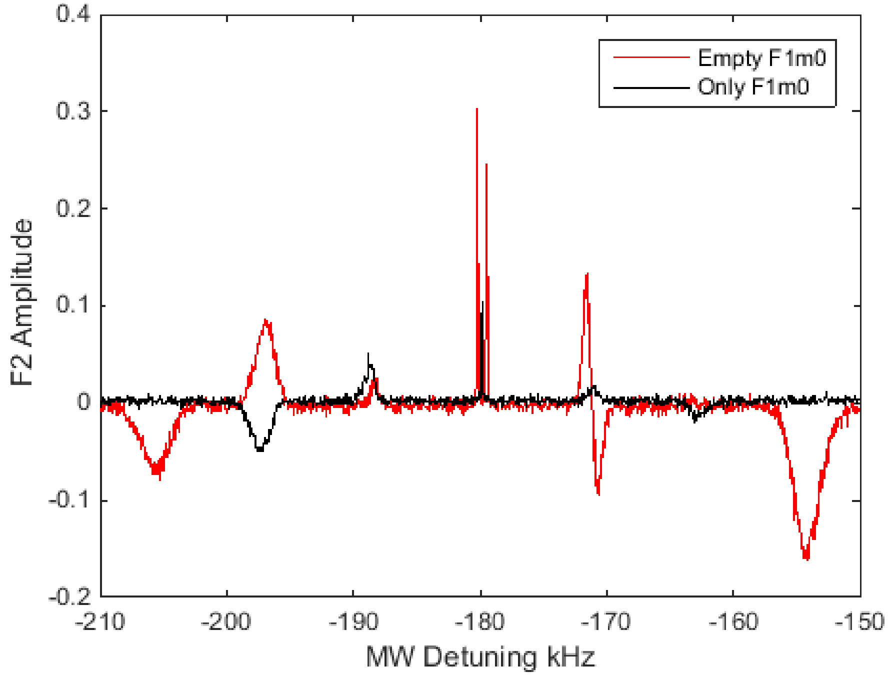

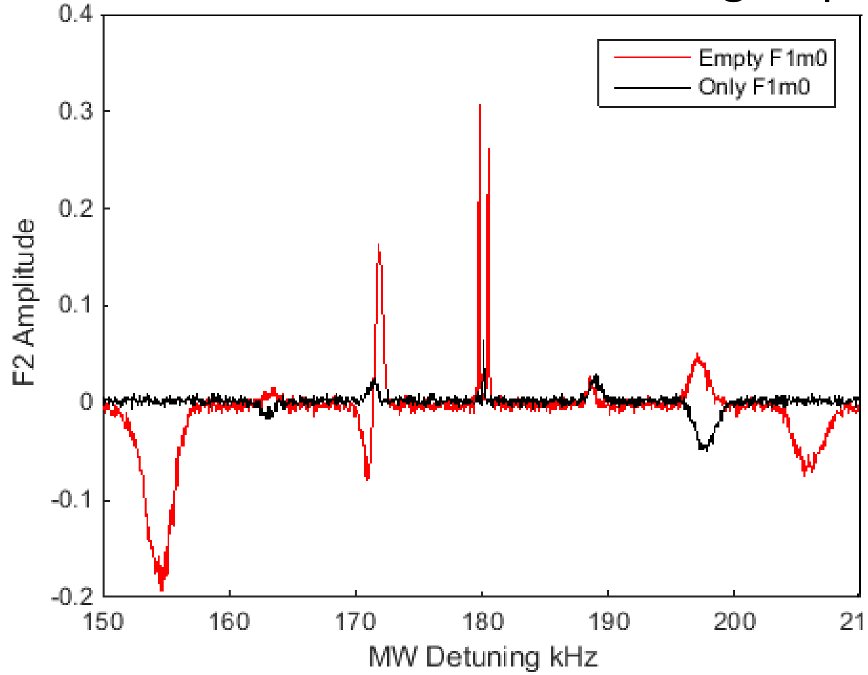

“Clock” triplet

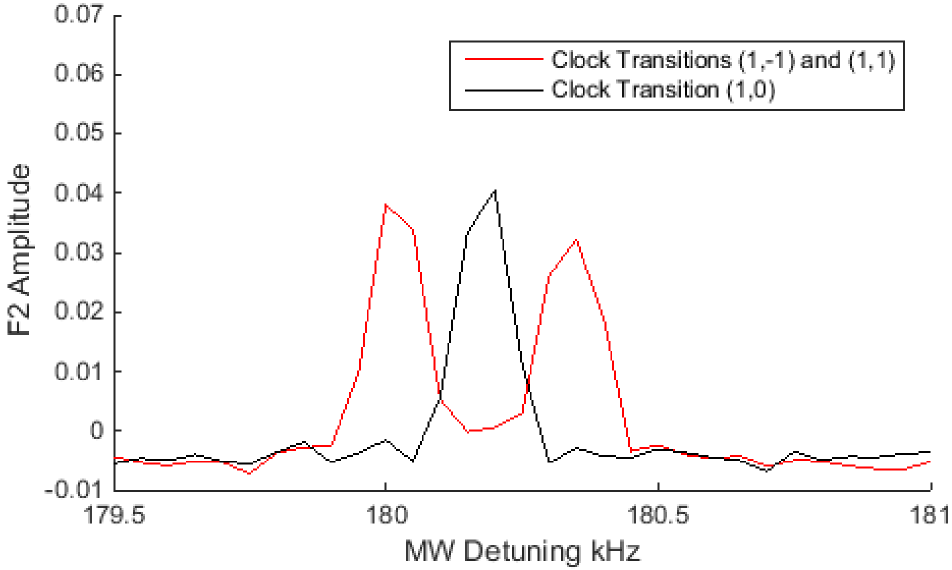

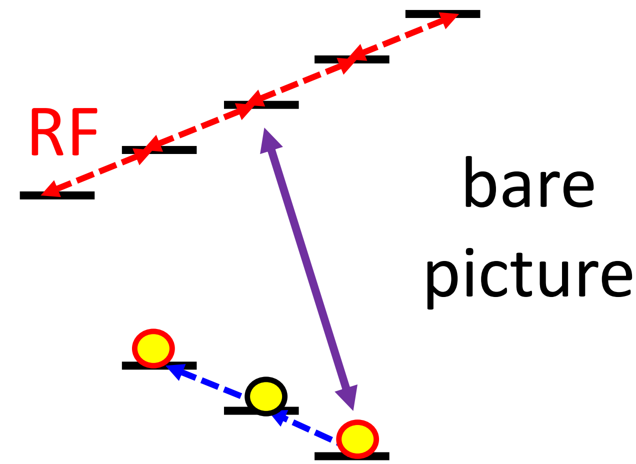

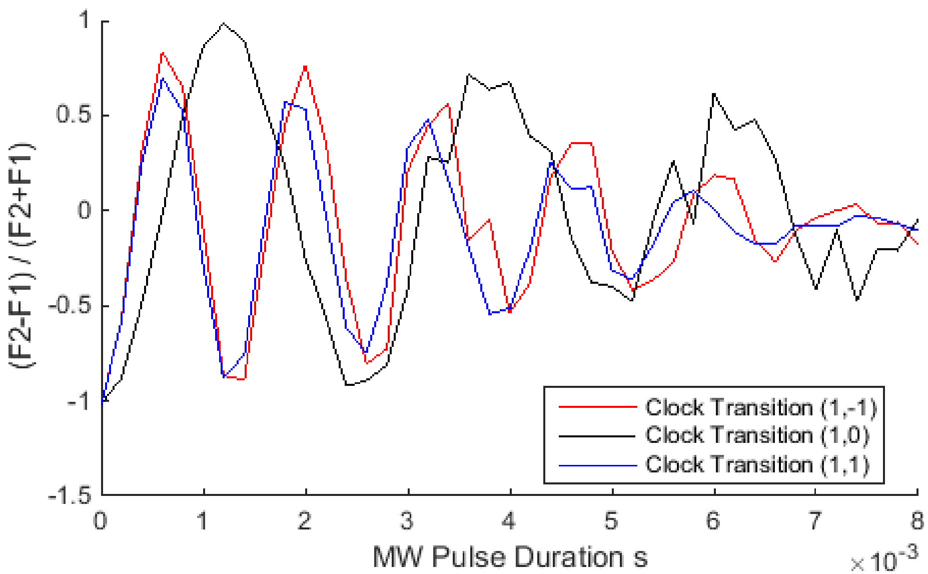

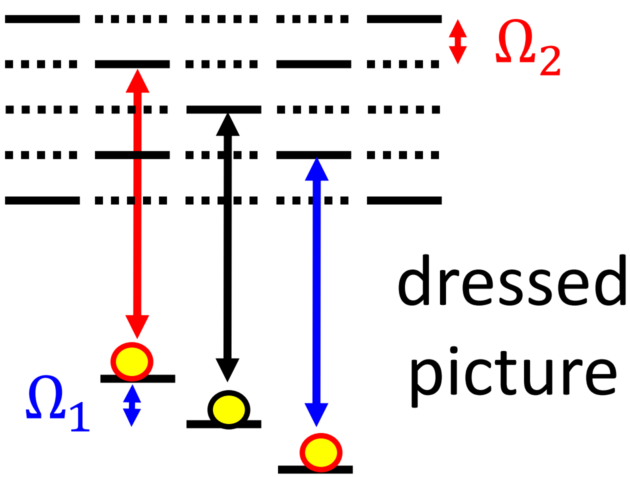

Field dependence

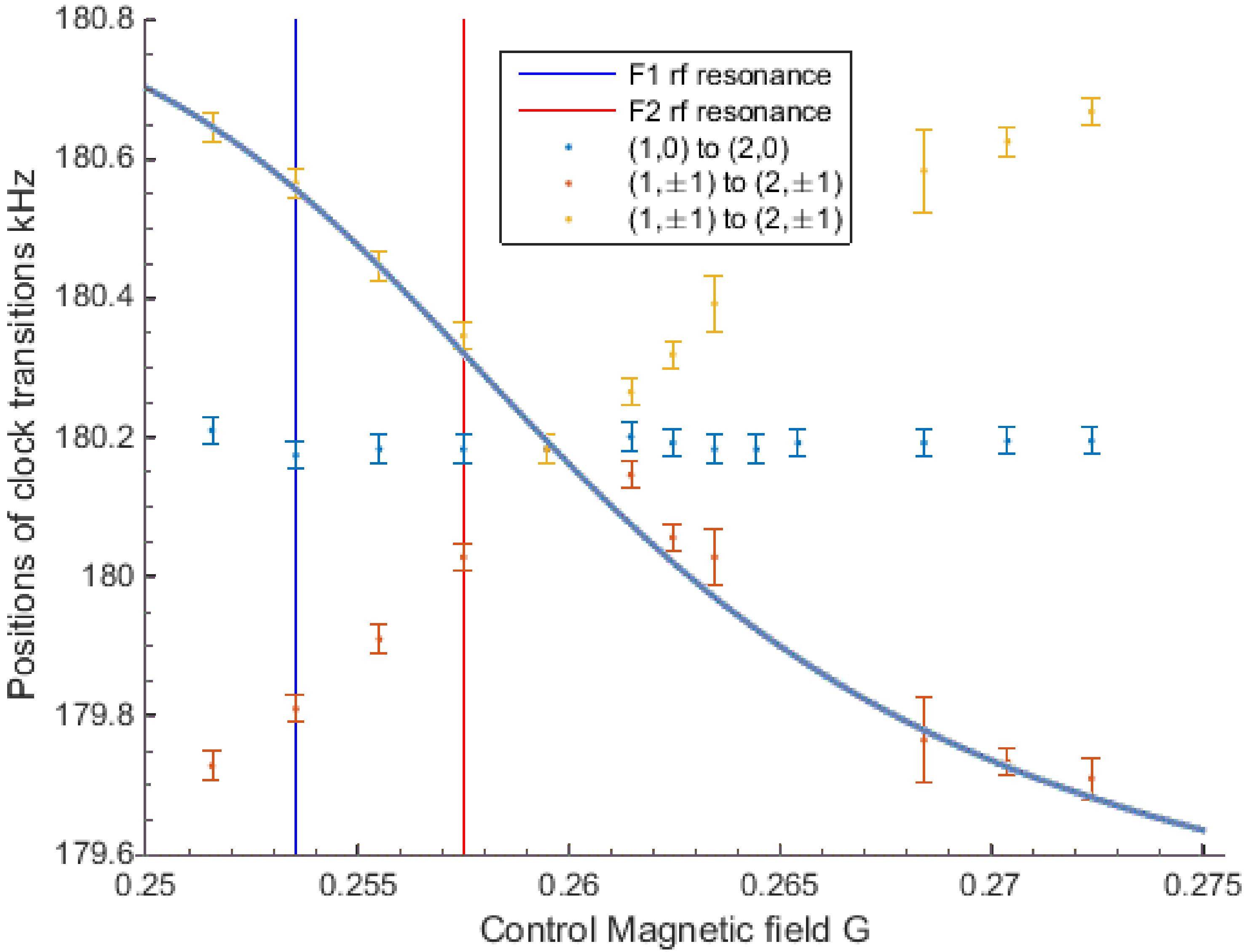

Inferred Dressed Potentials

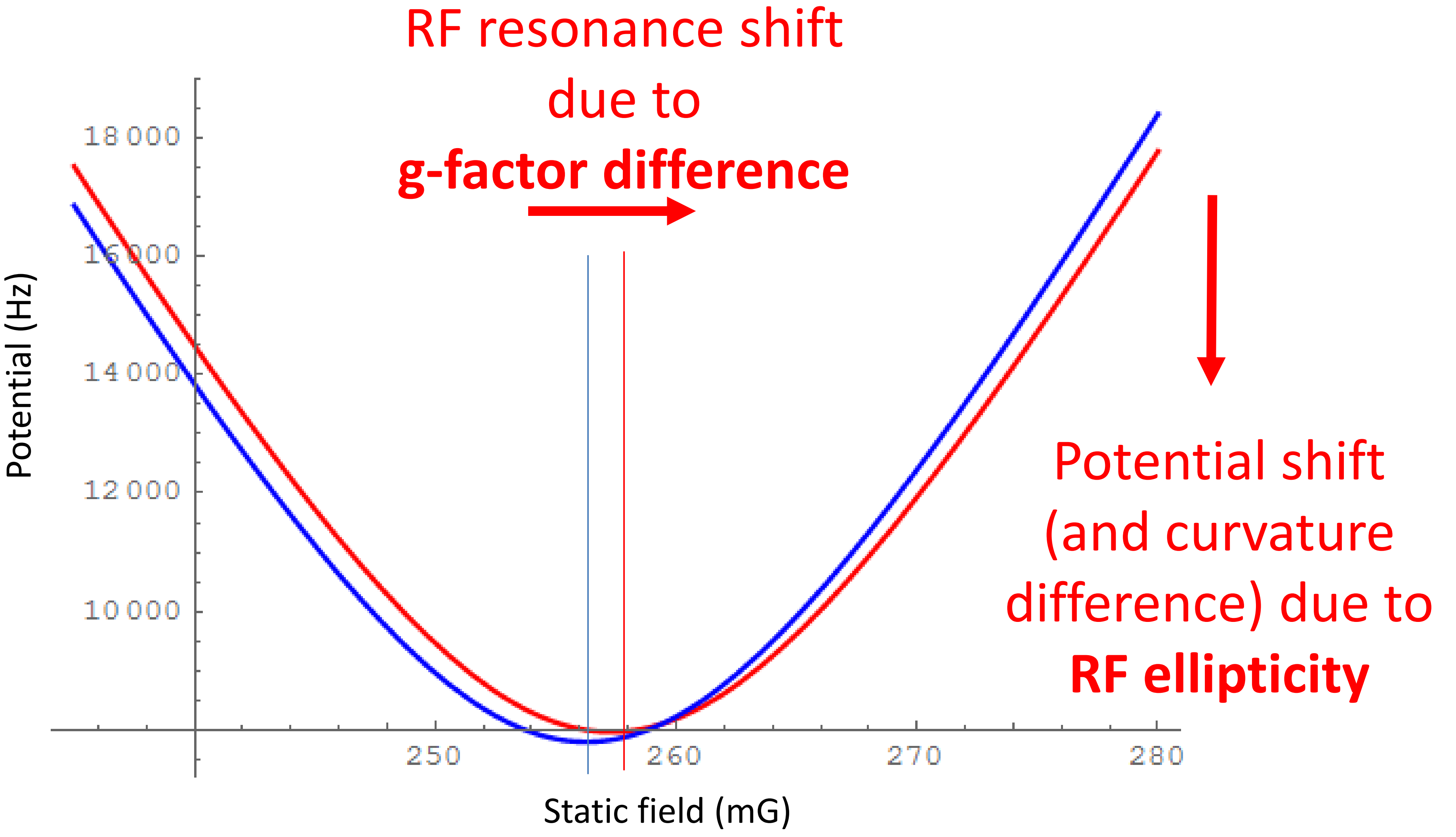

Ideas and Questions

- Equalize potentials

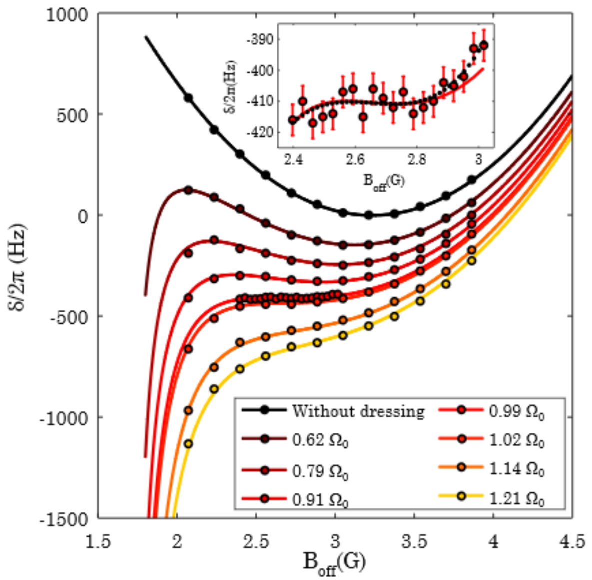

- MW/RF dressing (see talk by József Fortágh), but with RF dressed potentials, robustness?

  PRA **90**, 053416 (2014), also PRA **91**, 023404 (2015)

- Separate frequencies (see talk by Wolf von Klitzing), requires radial or vertical currents in this setup

- Topological constraints for dressed traps?

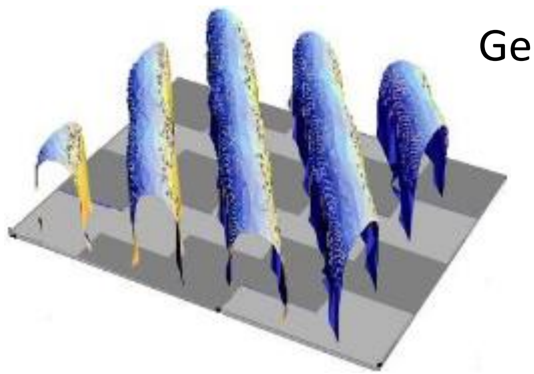

Gerritsma, Spreeuw, PRA **74**, 043405 (2006)

- 2D periodic boundary conditions
- Lattices of rings & ring lattices
- Artificial gauge fields in dressed lattices?
- Non-adiabatic potentials?